SAND79-0422
Unlimited Release

A Methodology for Determining the Configuration of the Optimum Solar Total Energy System

Ralph R. Peters

Prepared by Sandia Laboratories, Albuquerque, New Mexico 87185 and Livermore, California 94550 for the United States Department of Energy under Contract DE-AC04-76DP00789

Printed May 1979

Sandia Laboratories
energy report

SF 2900

Issued by Sandia Laboratories, operated for the United States Department of Energy by Sandia Corporation.

Printed in the United States of America

Available from
National Technical Information Service
U. S. Department of Commerce
5285 Port Royal Road
Springfield, VA 22161

Price: Printed Copy $4.50 ; Microfiche $3.00

SAND79-0422
Unlimited Release
Printed June 1979

A METHODOLOGY FOR DETERMINING THE CONFIGURATION OF THE OPTIMUM SOLAR TOTAL ENERGY SYSTEM

Ralph R. Peters
Systems Analysis Division 4723
Sandia Laboratories, Albuquerque, NM 87185

ABSTRACT

This paper presents a methodology for determining the configuration of the most economical Solar Total Energy System (STES) for a particular application. This methodology also can be used to design Small Power Systems and Solar Process Heat Systems because they are special cases of a STES. Since the values of the economic parameters used in this analysis are not well-defined, restrictions can be placed on the amount of purchased electricity and fossil fuel. Using these restrictions, one can design, for example, the most economical STES which purchases one-fourth as much energy as a conventional system. The results of the analysis include the system design, its performance, annualized cost, etc., and polynomials which can be used to determine system cost and energy purchases at off-optimum design points.

The results of an investigation of an application similar to the Bleyle Plant in Shenandoah, Georgia (the site of Large Scale Experiment #2), are presented. The sensitivity of the results to changes in the energy inflation rates, the electricity pricing schedule, system location, and restrictions on the amount of purchased energy were investigated in this study. The results indicate a STES which starts operation in 1982 is competitive for this application. In many cases it is less expensive than a conventional system which purchases all of the electricity and fossil fuel required to satisfy the application's demands. These results are based upon high production rate costs for the major components.

ACKNOWLEDGMENTS

The author would like to especially acknowledge the contributions of two individuals: E. A. Aronson (2623), who converted a set of ideas and equations into a usable computer code, and W. P. Schimmel (4723), for his comments on this paper.

CONTENTS

FIGURES

TABLES

A METHODOLOGY FOR DETERMINING THE CONFIGURATION OF THE OPTIMUM SOLAR TOTAL ENERGY SYSTEM

Introduction

The advent of the recent "energy crisis" has made it apparent that all possible energy sources must be utilized to their fullest potential. This, coupled with a desire to minimize the thermal pollution to the biosphere, makes the concept of total energy very attractive. In the early days of the total energy concept it was referred to as the cascaded energy scheme. Waste heat which was conventionally rejected to either the atmosphere or some convenient body of water was used to provide space, hot water or industrial process heating. According to the second law of thermodynamics, the idea of closely matching the source temperature of the working fluid with the application provides minimum entropy generation and thus is inherently a better use of the energy. This concept applies to any power generation system which has a heat engine, but it is especially true in the case of solar energy. In the following discussion, the total energy system utilizing solar energy will be referred to as the STES. In the solar collector field a circulating fluid (e.g., Therminol 66) is heated by solar radiation to a mid-range temperature (e.g., 320°C). This high temperature fluid is then used to power a Rankine-cycle engine. A STES turbine is designed so that, in addition to producing electricity, it utilizes turbine reject heat to meet the process heat needs of the application. Solar energy utilization is dependent on many factors, but is typically quite high (e.g., 75%), although the solar to electrical conversion efficiency could be on the order of 25%. The reason for this is that the use of reject heat displaces fossil fuel which would normally be used to meet the process heat demands.

The design of a STES for a particular application is fairly difficult, since there are many options to consider. The STES could be a hybrid system where a substantial fraction of the energy demands are met by conventional sources (e.g., electricity purchased from the public utility), or it could be a stand-alone system. Sizing of the components likewise involves many options. The collector field can be sized so that it will provide the required electrical and/or thermal energy for most of the year. However, if this design were selected, it would probably not be very efficient during the summer. The collector field might instead be designed to meet the application's energy needs during the summer only. This system would have to be supplemented by other energy sources during the remainder of the year. Similarly, there are many sizing options for the thermal energy storage which could be used as buffer, overnight, or weekend storage.

For these reasons, STES are usually designed in a piecemeal fashion. Based upon the energetics discussed above, the solar collectors might be sized, for example, to meet all of the energy needs of the application during the summer only. The cost of energy provided by thermal storage is typically constant for small storage sizes, but as the size is increased the cost will, at some point, increase dramatically. Based on this consideration alone, the size of thermal storage would be chosen at a value slightly less than that at the knee of the energy cost versus size curve. The sizes of the other components are usually determined in a similar manner. There is, however, no guarantee that a system designed with these components would be anywhere near optimum.

An economic analysis of a STES designed in this manner almost always finds the energy provided is much more expensive than that available from conventional sources. This indicates a STES which is designed in a piecemeal fashion is not economical; however, it should not be taken to mean that STE systems cannot be made economical for many applications. Obviously, what is needed is a series of system components which have been optimized when their interaction and system performance are considered.

The piecemeal design and other similar methodologies have several basic problems. The first is that in designing the STES they use a set of rules which is probably not economically valid for a substantial fraction of the applications. The second is that the system is designed in modules, which is generally not a satisfactory way to achieve an optimized system. Finally, they simply cannot investigate the whole spectrum of possible STE systems and therefore their design probably will not be the most economical.

These and other problems indicate that it would be desirable to have a methodology which would design a STES subject only to the restriction that it would provide all of the required energy at the lowest possible cost. Since the values of the economic parameters are not well defined, it would be desirable to be able to place restrictions on the amount of electricity and fossil fuel purchased. This could be used to determine, for example, the design of the most economical STE system which would purchase 25% of the energy that a conventional system requires. The remaining 75% would be provided by the solar collectors.

The purpose of this paper is to describe such a methodology and indicate some results obtained using it to design a STES for a particular application. The sensitivity of the system design to changes in economic parameters, system location and limits on the amount of purchased energy will also be discussed.

System Model

In order to design the optimum system one must start with an accurate system model. In addition, the model must be flexible so that a wide variety of applications can be investigated. These requirements conflict with the other constraints; namely, that the computer space required by the numerical model should be reasonably small and the system simulation should require very little computer time. The latter constraint is necessary so that many different system configurations can be investigated. The model accuracy and flexibility requirements along with the computer time and space constraints have played a major role in shaping the development of the numerical model.

The model is flexible so that it can be used to design STE systems for many different applications. In order to satisfy the energy demands of any application STE systems are allowed to obtain energy from several sources, which include 1) the sun (as solar radiation), 2) fossil fuels (e.g., coal, oil and gas) and finally, 3) electricity from a public utility. The model is also very flexible in the manner in which it considers energy demands. Energy can be provided as 1) process heat (at three different temperatures), and 2) electricity. By adjusting these energy demands the STE system can become, for example, 1) a power plant which generates electricity for a public utility, 2) a total energy system which provides electricity, heating, and cooling for a high rise apartment building, 3) a total energy system which provides process heat and electricity for a food processing plant, or 4) a solar process heat system which provides process steam for food processing.

A large number of components have been included in the STE system to provide additional flexibility. There are eleven independent components whose sizes may be independently varied in order to determine the most economical (optimum) system design. These include 1) four collector types (high temperature thermal, low temperature thermal, photovoltaic, and concentrating photovoltaic), 2) three energy storage types (high temperature thermal, low temperature thermal, and battery), 3) three types of turbines, or up to a three-stage turbine (high, intermediate, and low pressure), and 4) a gas turbine. Because the division of the cooling load between an absorption refrigeration unit and a vapor compression unit can affect system economics, a twelfth optimization parameter has been included. This parameter allows the division of a cooling load (the AR/VCR load) between the two refrigeration units to be varied, so that the optimum system design can be determined. In order to maintain maximum flexibility, two other cooling loads also may be specified; one which can be satisfied by only the absorption unit, and another which can be satisfied by only the vapor compression unit. The remaining dependent components (e.g., the condensor and cooling tower) are sized for efficient system operation. The components and their functional relationships are shown in Figure 1. It should be mentioned that the size of any component may be zero for a particular application or may shrink to zero for a particular set of economic conditions. For example, if the cost of electricity and fossil fuel were relatively low, the size of the solar collector field could shrink to zero in order that the energy be provided at the lowest possible cost.

Solar collectors are an important component in STE systems. Two different classes are identified in Figure 1; high temperature and low temperature collectors. The high temperature collectors provide energy which is ultimately used in the heating of the thermal engine's working fluid. Depending upon the fluid temperature of the collectors and the required state conditions, energy from these collectors may be used to 1) heat feedwater, 2) heat feedwater and vaporize the working fluid, or 3) heat feedwater, vaporize and superheat the working fluid. If, at some instant, more energy is being collected than the system

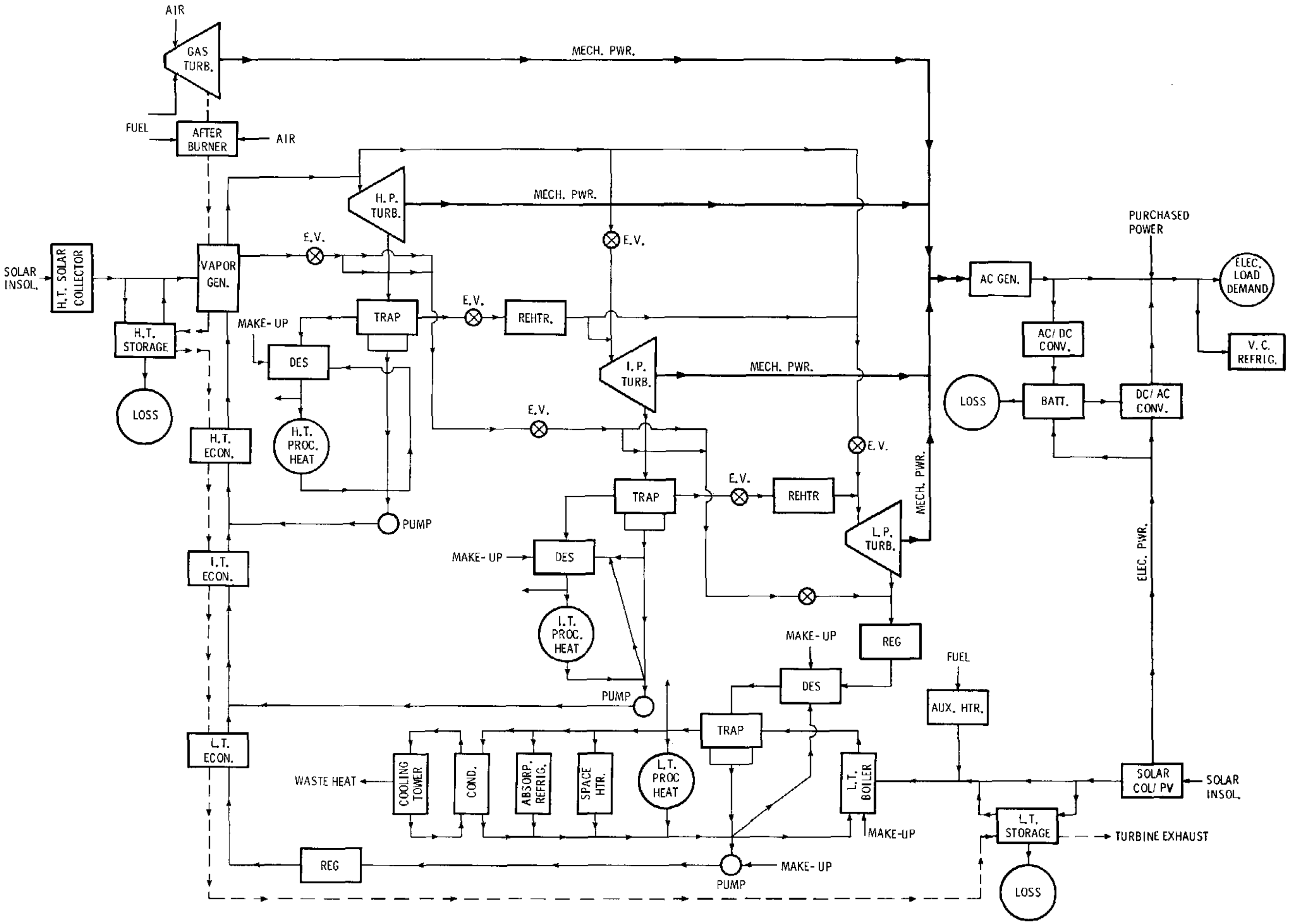

Figure 1. Solar Total Energy System

requires, the excess energy can be stored at high temperature for later use. The gas turbine and afterburner provide a backup for the high temperature collector and storage system.

The low temperature collectors provide low temperature thermal energy (and possibly electrical energy) for use by the STE system. The low temperature thermal energy can be supplied by the low temperature thermal collector field and the concentrating photovoltaic collector field. It is ultimately used to satisfy some portion of the heating, cooling, and low temperature process heat requirements. If more thermal energy is being collected than the system requires, the excess is stored at low temperature for later use. If the low temperature collectors and storage are unable to supply the necessary energy, heat can be supplied by the high temperature vapor generator. If this isn't possible, the auxiliary heater can be started to supply the necessary energy.

If the low temperature collectors are photovoltaic or concentrating photovoltaic collectors, they will also provide DC electricity to assist in satisfying the electrical energy demand placed upon the system. Components associated with the use of this electricity include batteries, for storage, an AC-DC convertor and a DC-AC convertor. If the STES cannot meet the electrical demand, power can be supplied by a public utility.

The types of collectors available include central receiver or distributed collector systems. The types of distributed collectors that could be chosen include parabolic trough collectors, paraboloidal dish collectors and flat plate collectors. The operation of these collectors is fairly flexible. For example, the parabolic trough collectors may be set up for either East-West axis tracking or for North-South axis tracking. If the collector is set up for North-South axis tracking, the collector can have a horizontal rotation axis or a polar axis mount.

The collector simulation is fairly sophisticated--solar energy available to the collectors is calculated using the solar energy availability equations of E. C. Boes.[1] The thermal energy collection efficiency is calculated using the equation

$$\eta_T = b + a \frac{T_{FIELD} - T_{AMBIENT}}{I}$$

where a and b are experimentally determined, T_{FIELD} is the average field temperature, $T_{AMBIENT}$ is the surrounding air temperature and I is the insolation rate. This equation is fairly valid for moderate field temperatures (e.g. 400°C). Both $T_{AMBIENT}$ and I are read from weather tapes on an hourly basis. The photovoltaic and concentrating photovoltaic units' electrical energy collection efficiency is assumed to be constant. The pumping power required to circulate fluid through the collectors is estimated using the equation:

$$\text{Pumping Power} = K_p Q$$

where K_p is the pumping power coefficient and Q is the amount of thermal energy being collected by the field.

A gas turbine and afterburner have been included in the STES to provide flexibility in the sizing and the operation of the high temperature collector field. If they had not been included, the high temperature collector field's minimum size would be that required for the production of enough thermal energy to satisfy the high and intermediate temperature thermal energy demands. As a result of including these components in the system, the collector area, for example, could be set to zero and the thermal demand would still be satisfied. The demand, in this case, would be met by using the high temperature gas turbine and/or the afterburner. This would be accomplished by routing the exhaust gases through the high temperature vapor generator, and the economizers.

The use of the gas turbine and/or afterburner exhaust also allows the temperature requirements to be satisfied as the fluid temperature of the collector field is varied. This flexibility can result in more economical performance. For example, a STES might be required to provide 425°C superheated steam. This requirement would heavily penalize a distributed collector system that lacked a gas turbine or an afterburner because the collector field would have to operate at a very high temperature (≈450°C) and would therefore have a low efficiency. In fact, flat plates and line focus systems probably could not provide fluid at this temperature. Systems which have a gas turbine or afterburner could use the high temperature exhaust to superheat the steam and therefore would be able to operate the collector field at a lower temperature and hence higher collector efficiencies.

Rankine cycle turbines are used to convert the working fluid's thermal energy into mechanical energy which is then converted into electrical energy by an AC generator. These turbines are operated at three different pressure levels to 1) increase the efficiency with which the thermal energy is converted into mechanical energy (by the use of cascading and reheat) and 2) provide for the possibility that process heat may be required at three different temperatures. If the low pressure turbine's reject heat is being used to satisfy the heating, cooling, and low temperature process heat requirements, excess energy may be stored at low temperature for later use.

The operation of the turbines is determined by specifying the inlet and outlet enthalpies and the turbines' duty cycles. Any sort of working fluid (e.g., water, toluene, freon) may be used in the numerical simulation if property tables are available for the fluid. A regenerator is included in the model as it would be in actual installation to increase total system efficiency. The power required for condensor and cooling tower operation is estimated in a manner similar to that used to estimate the collector field's pumping power.

Economics

The basis for determining which STES is the optimum one is the annualized system cost. The annualized system cost can be considered the average annual payment that would be required to keep the system in operation. It is a function of the capital cost of the system, the annual cost of purchased electricity and fossil fuel, the annual operation and maintenance cost and a large number of economic parameters. They specify, for example, the effective income tax rate, electricity and fossil fuel cost inflation rates, and the system lifetime. The methodology used is essentially that developed by A. M. Perino.[2]

Optimization

The objective of the optimization section is to determine the configuration of the STES which has the lowest possible annualized cost and is able to provide the energy required for the application. If there were only two optimization parameters, instead of twelve, one could visualize this problem as one of finding the lowest point on a surface which is bounded on all four sides. This point will be referred to as the "global" minimum. It is apparent that this surface may have many local minima in it, and therefore a pattern search routine, like MINA,[3] may find a large deep local minimum instead of the global minimum. This problem is not unusual for the case where MINA is searching a twelve-dimensional surface for the global minimum (optimum STES).

One solution to this problem is to gather information about the general shape of the surface and then start the search routine at the point where the global minimum is thought to occur. The search routine should then find the global minimum.

The methodology for estimating the point at which the global minimum occurs has three steps. The first step involves gathering information about the entire surface by means of a Latin Hypercube Search (LHS). The LHS is a directed random search which puts a large number of randomly designed systems together for evaluation. The LHS is preferred because it assures uniform coverage of the surface and so it insures that the maximum amount of information is gathered for a certain number of points. The only restrictions on these systems are that the optimization parameters be within a specified range and the electrical generation capacity must be less than or equal to the peak electrical demand. The operation of these systems is then simulated and the annualized cost, fossil fuel and electricity purchases are determined. The result is a table listing the sizes of the twelve optimization parameters, the annualized cost and the annual fossil fuel and electricity purchases for each system.

The second step generates quadratic polynomials for the annualized cost (C) and annual fossil fuel (Q) and electricity (E) purchases. The data generated in Step 1 are used by a stepwise regression code to generate the quadratic polynomial which accurately estimates the value of the quantity in question as a function of the twelve optimization parameters but does not overfit the data. The methodology cited in Steps 1 and 2 is similar to that used by R. L. Iman.[4]

The objective of Step 3 is to find the quadratic polynomial's global minimum subject to several constraints. The available area is always constrained by the ranges of the optimization parameters (typically zero to some value for the eleven component size optimization parameters and zero to one for the AR/VCR load optimization parameter). The installed electrical generation capacity must also be less than or equal to the peak electrical demand. Another possible set of constraints concerns the amount of fossil fuel purchased annually and the amount of electricity purchased annually. If a conventional system is defined as one with no solar collectors, energy storage or turbines and the entire AR/VCR cooling load satisfied by the vapor compression refrigeration unit, and if the annual amount of fossil fuel and electricity purchased are denoted by Q_c and E_c respectively, then the constraints which may be placed on the STES are:

1) $Q/Q_c < X$

2) $E/E_c < Y$

3) $\frac{(Q + E)}{(Q_c + E_c)} < Z$

where X, Y and Z are non-negative real numbers.

Currently a large number of randomly sized systems which meet all the restrictions are assembled (e.g. 1000) and then evaluated using the C, E and Q polynomials. The result is the lowest cost system. It is a fairly accurate estimate of the point at which the cost polynomial's constrained global minimum occurs. This point is used as a starting point for MINA which will then find the optimum system configuration subject only to the accuracy of the LHS methodology estimate.

An indication of the usefulness of the LHS technique can be made by comparing the results of some cases where MINA was started at the LHS point and others where MINA was started at an arbitrary point (the point where the sizes of the relevant optimization parameters were one-half their maximum allowable value). Thirty different cases were run and in only one case was the LHS result significantly worse than the result obtained when MINA was started at the 50% point indicated above. A further breakdown shows the following:

$(C_{50\%}-C_{LHS})/C_{LHS}$	No. in Range
-.14	1
-.024	1
(-.01, .01)	13
(.01, .05)	2
(.05, .10)	7
(.10, .15)	2
> .5	2

where the subscript on C refers to MINA's starting point. In two cases MINA, when started at the 50% point, was unable to find a design which met the restriction on the quantity $(E + Q)/(E_c + Q_c)$. In two other cases the 50% point result was significantly more expensive than the result when MINA was started at the LHS point.

The polynomials resulting from the LHS methodology are quite useful. They show the sensitivity of C, Q, and E to changes in the values of the optimization parameters. In fact, they make a classical sensitivity study quite easy. It is simply a matter of determining the functional form of a few partial derivatives. In addition, it is quite simple to determine the effect of a change in the design. All that is required are the C, E and Q polynomials and a four function calculator.

Results

In order to demonstrate the usefulness of this methodology, one application has been thoroughly investigated. The application chosen is the Bleyle Plant in Shenandoah, GA. This case was chosen because it is the site for Large Scale Experiment #2,[5,6] and thus most of the information needed for application of this methodology is available in the General Electric contractor reports. The load data used are based upon information contained in these reports. Plots of the values used are shown in Figures 2-5. Since these values are defined on an hourly basis, there are slight differences between them and those found in the reports which are continuous functions of time.

The layout of the system used to supply the needs of this application is shown in Figure 6. The paraboloidal dish collectors along with the auxiliary heater (the afterburner of Figure 1) provide the thermal energy required to meet the process heat needs of the application and operate the turbines. The thermal efficiency of the collector field is estimated from the equation:

$$\eta = .8041 - \frac{.00019\left(625 - T_{AMBIENT}\right)}{I}$$

where $T_{AMBIENT}$ is in °F and I is in kW/m^2. This equation accounts for both collector and field losses. The values of the constants were obtained from GE reports. The field pumping power coefficient is .0178. Some of the outlet steam from the high pressure turbine stage is used to satisfy the process heat needs. The reject heat from the low pressure

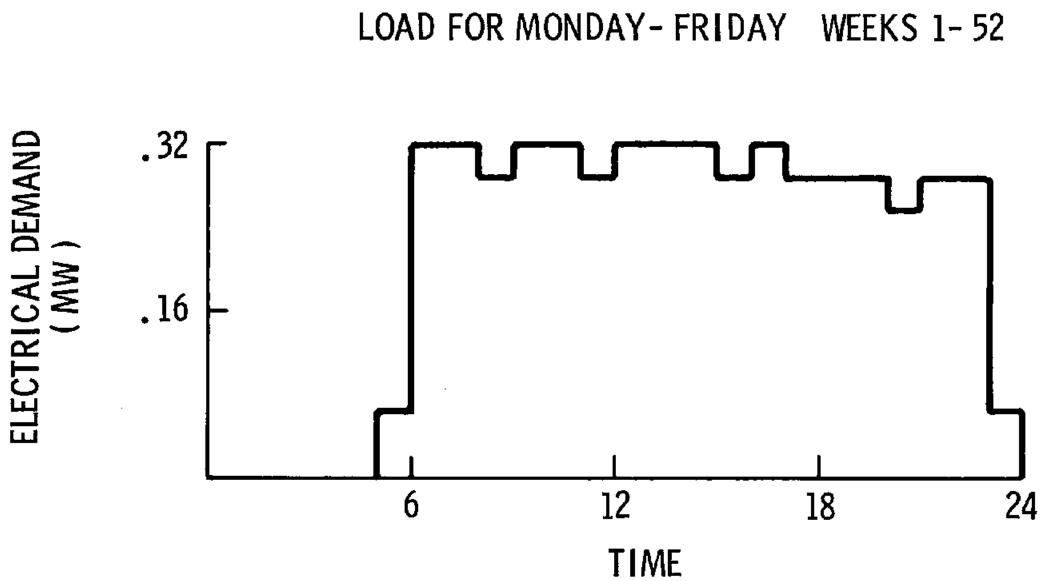

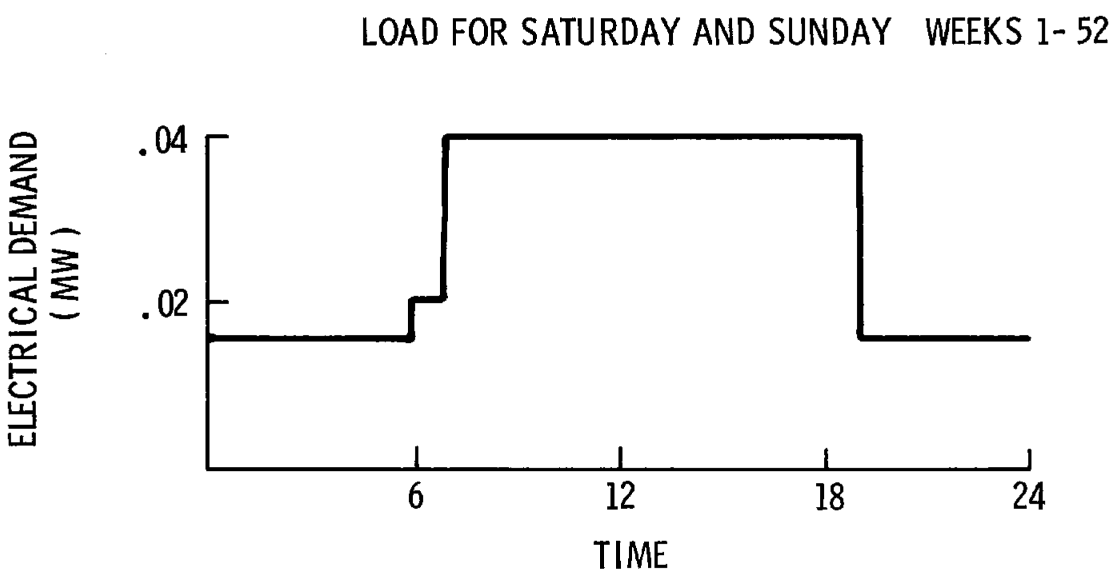

Figure 2. Electrical Demands

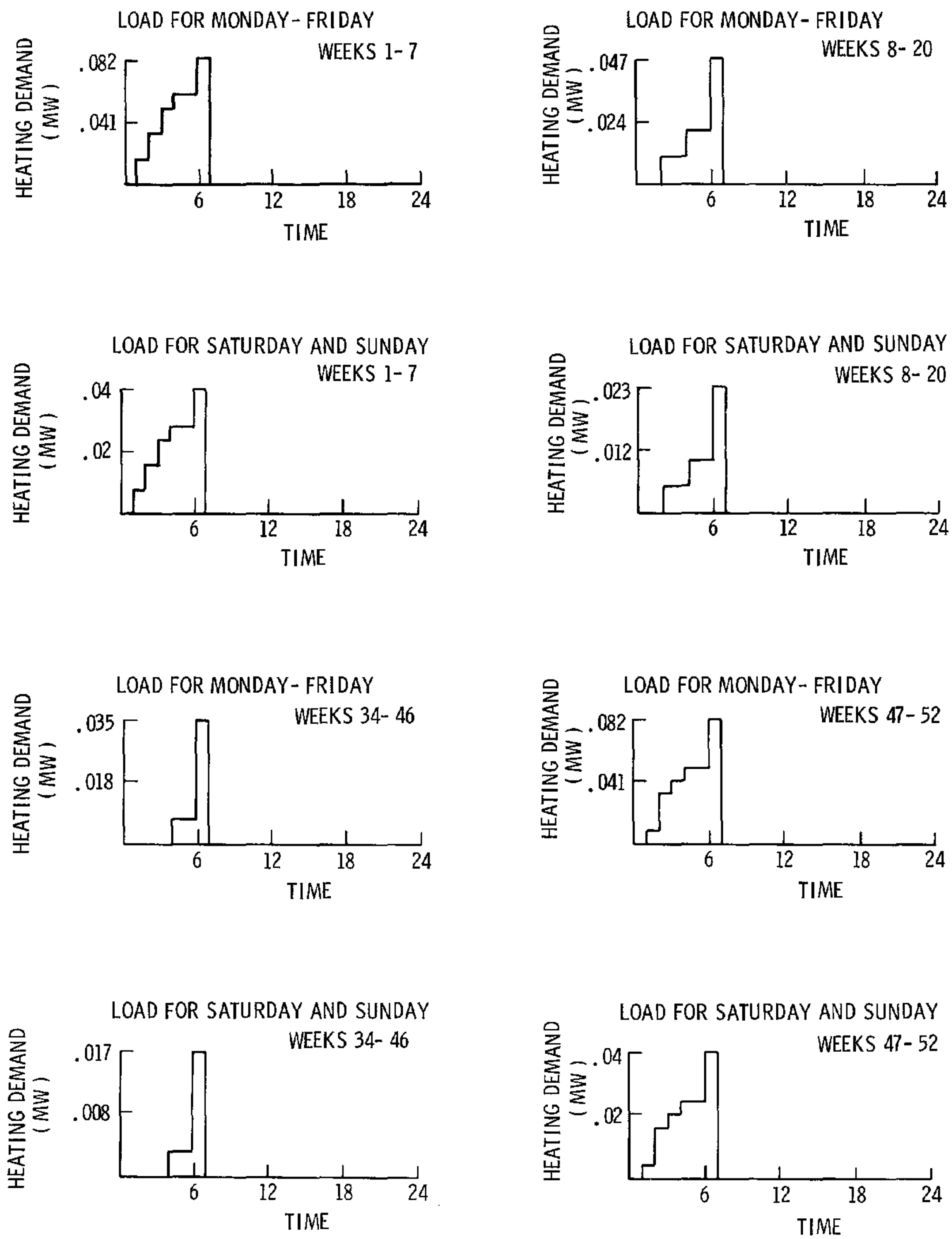

NOTE: ZERO DEMAND FOR WEEKS 21- 33

Figure 3. Space Heating Demands

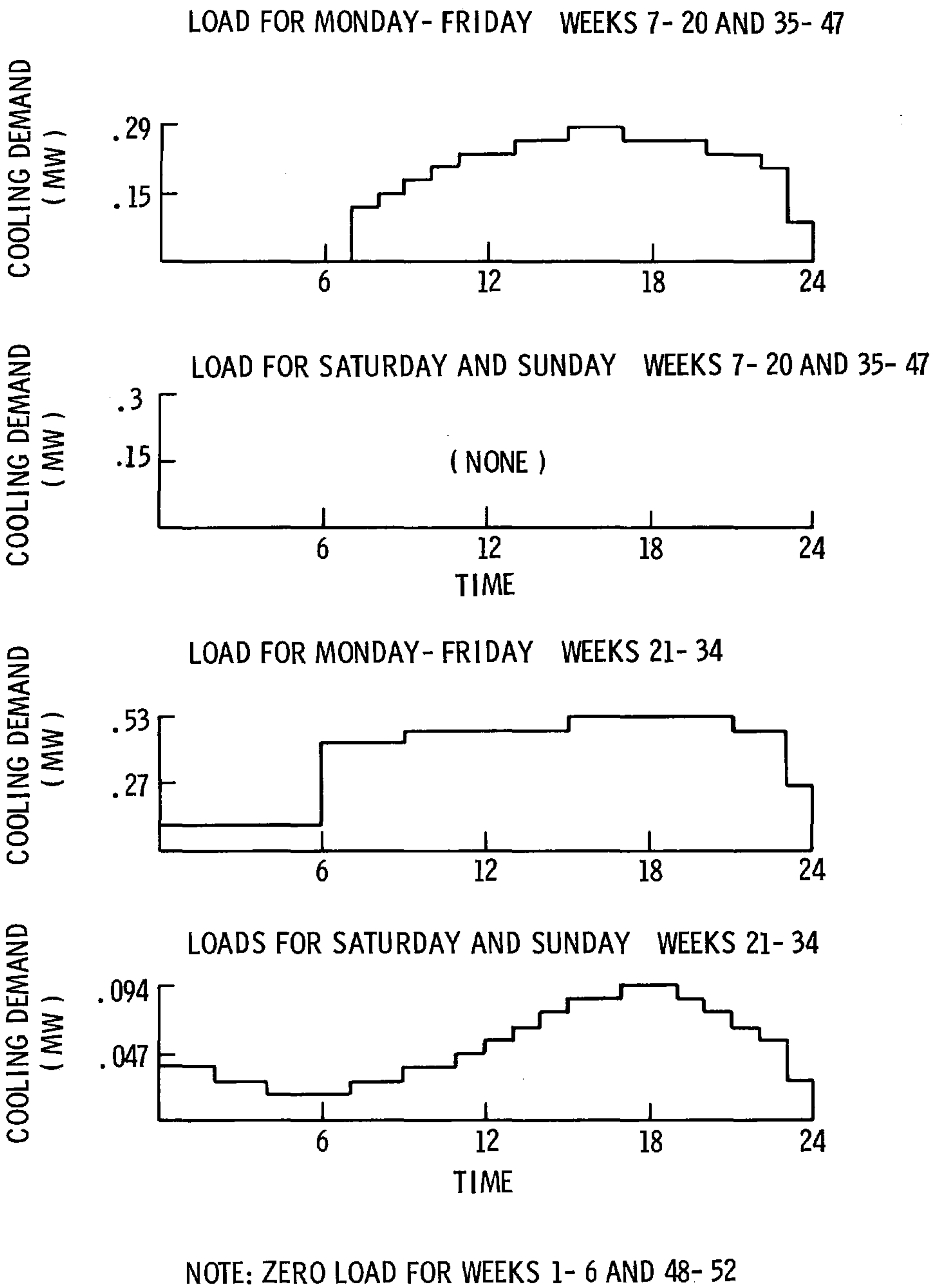

Figure 4. Airconditioning Demands

LOAD FOR MONDAY-FRIDAY WEEKS 1-52

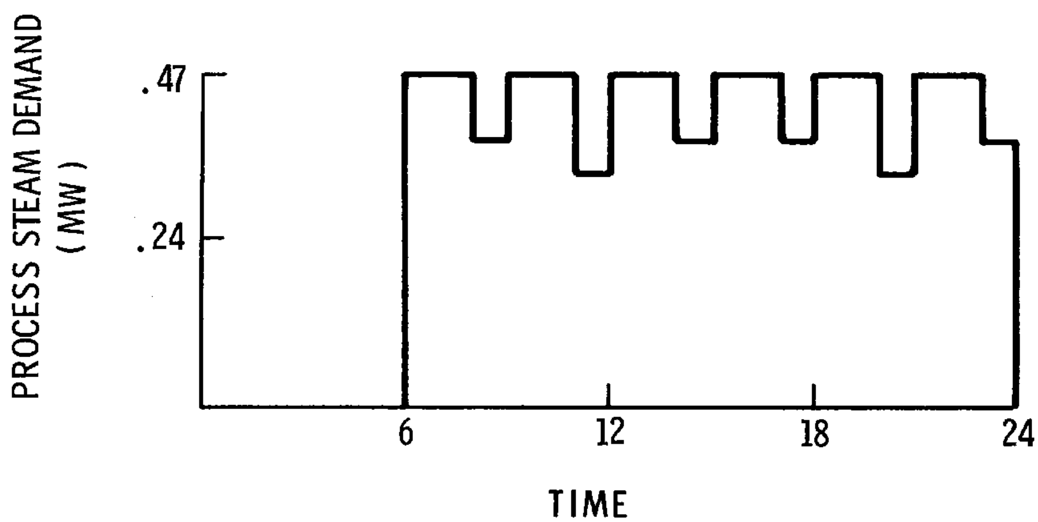

NOTE: ZERO LOAD SATURDAY AND SUNDAY.
.47 MW CORRESPONDS TO 1380 LBS/HR
OF 120 psia SATURATED STEAM BEING
WITHDRAWN FROM THE SYSTEM.

Figure 5. Process Heat Demands

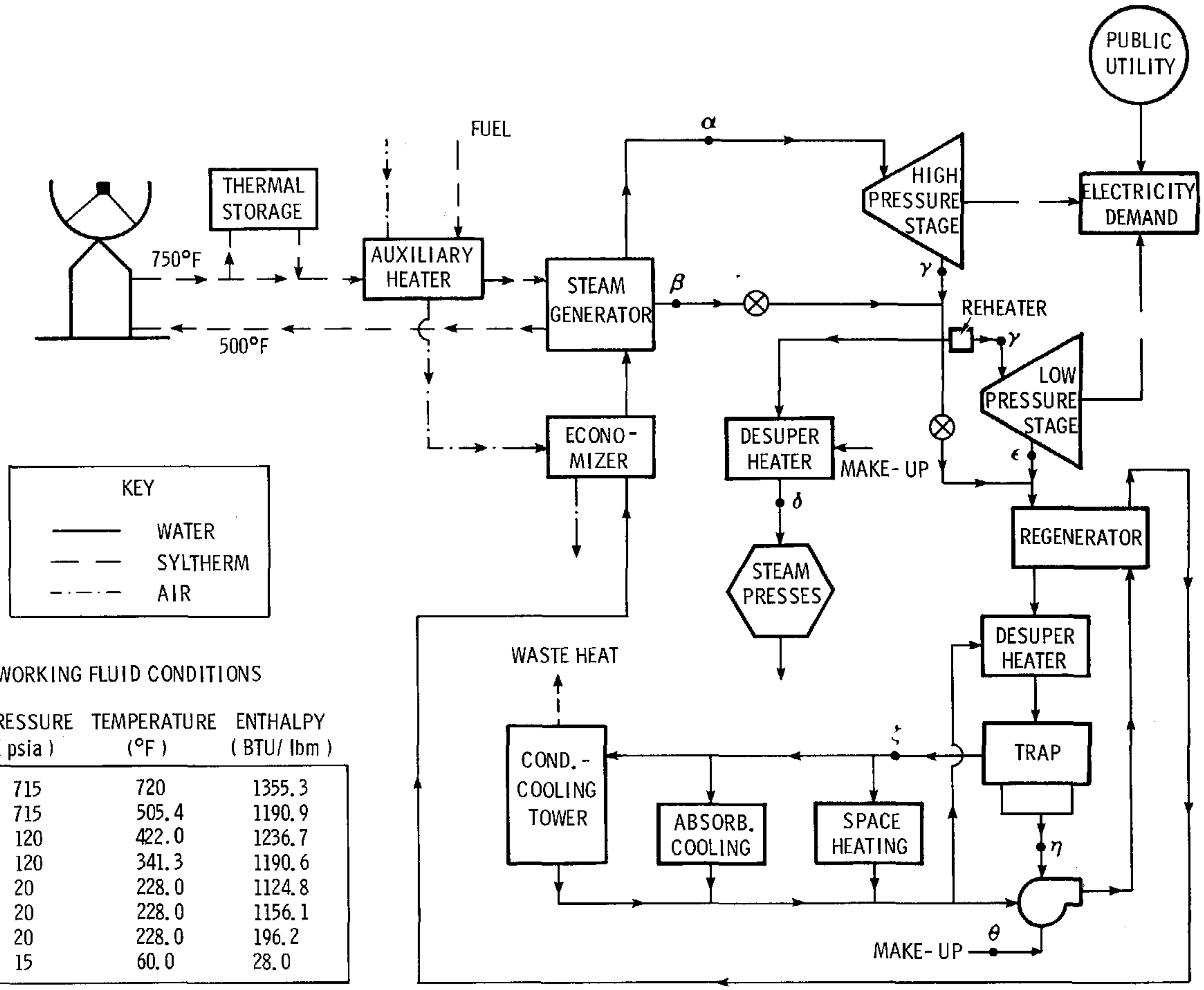

WORKING FLUID CONDITIONS

POINT	PRESSURE (psia)	TEMPERATURE (°F)	ENTHALPY (BTU/lbm)
α	715	720	1355.3
β	715	505.4	1190.9
γ	120	422.0	1236.7
δ	120	341.3	1190.6
ϵ	20	228.0	1124.8
ζ	20	228.0	1156.1
η	20	228.0	196.2
θ	15	60.0	28.0

Figure 6. System Configuration

stage is used to heat and cool the building. Electricity is provided by the turbines and may also be purchased from the public utility. Figure 6 also shows the conditions throughout the system. For example, the steam pressure at the inlet of the high pressure turbine stage is 715 psia, the temperature is 720°F and the enthalpy is 1355.3 Btu/lb. These values are based upon information contained in the GE reports[5,6] and information received from J. P. Abbin.[7] The turbine's duty cycle is shown in Figure 7.

The conventional system, which is the standard for comparison, uses the auxiliary heater to directly fire the steam generator. This is standard operation when there are no high temperature collectors and thermal storage. The steam generator provides saturated steam to satisfy the process heat demands. Part of the output of the steam generator is cooled to provide the thermal energy required for heating and cooling. The conventional system purchases electricity to satisfy the electrical demand.

Sensitivity to changes in economic conditions were investigated. Four different sets of economic conditions are defined in Table I. The values of most of the economic parameters for Case I were obtained from the GE reports.[5,6] The difference between Cases I and II and between III and IV are the inflation rates for electricity and fossil fuel. The cost of electricity for Cases I and II is constant, while for Cases III and IV it is variable. If all the electricity were purchased from the public utility, its annualized cost would be approximately the same for both price schedules; $85,800 and $82,400 for the constant and time-of-day price schedules with the low electricity inflation rate. The beginning year of operation for these systems is 1982.

The costing algorithms used for the collectors, storage and the turbine stages are listed in Table II. These algorithms were derived from information in the GE reports[5,6] and information received from J. P. Abbin.[7] They represent estimates on component costs for mature technology systems with a high production rate for the major components.

The sensitivity to system location was also investigated. The weather tapes used in this study are the Typical Meteorological Years (TMY).[8] Nashville, Tennessee was chosen for one location because a review of the available TMY stations indicated that the climate appeared to be most like that of Shenandoah, Georgia. Albuquerque, New Mexico

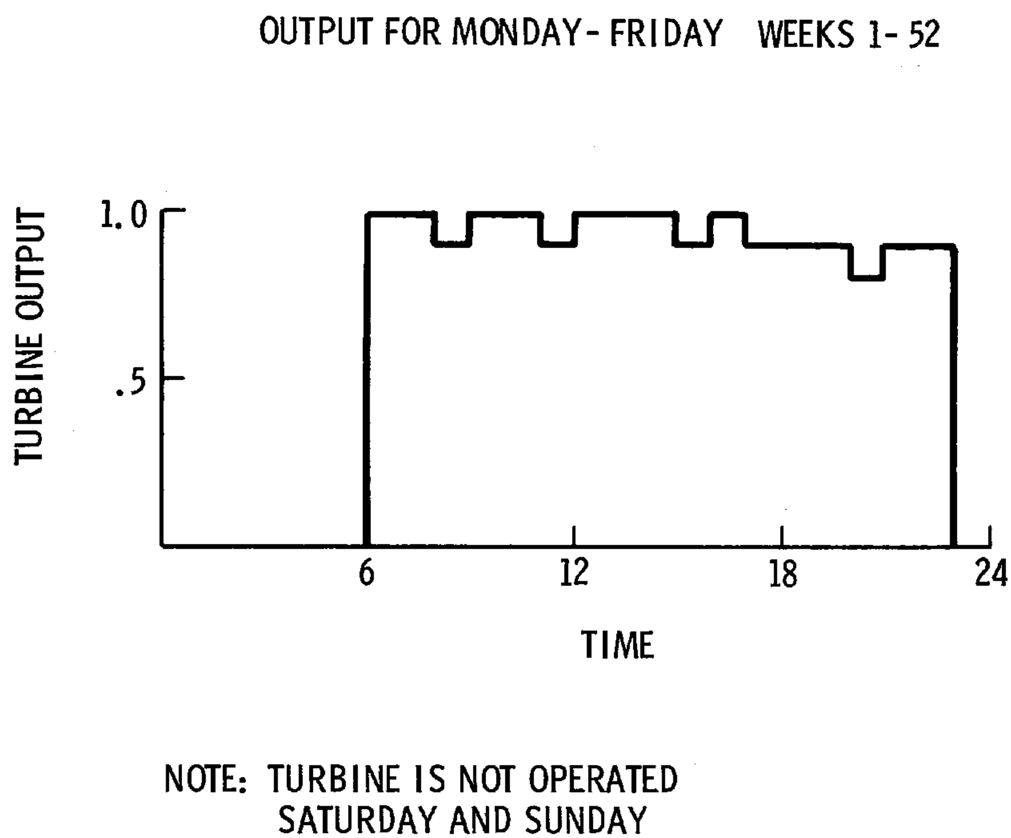

Figure 7. Turbine Duty Cycle

TABLE I. Economic Parameters

Discount Rate	12%
Interest Rate	9%
Property Tax Rate	0%
Downpayment	20%
Income Tax Rate	50%
Investment Tax Credit	20%
O & M as a Percent of Capital Cost	1.5%
Cost of Fossil Fuel	.6¢/kWh
General Inflation Rate	6%
Lifetime	20 years
Depreciation	Sum-of-Years Digits
Price Year	1978
Operation Year	1982

Case	I	II	III	IV
Electricity Cost Inflation Rate	10%	14%	10%	14%
Fossil Fuel Inflation Rate	12%	18%	12%	18%
Electricity Cost	4¢/kWh	*	4¢/kWh	*

*The time-of-day pricing scheme follows

	Daily Cost				Weekend Cost	
Weeks	Time (hr)	Cost†	Time (hr)	Cost	Time (hr)	Cost
1-8, 48-52	22-6	1.84	7-21	4.6	0-23	1.9
9-21, 34-47	22-6	2.34	7-21	3.9	0-23	2.2
22-33	19-10	2.01	11-18	6.7	0-23	2.0

†The cost is in units of ¢/kWh

TABLE II. Costing Algorithms for Major Components

Component	Cost (K$)
Paraboloidal Dish Collector	$250 \cdot \left[\text{Field Size } (10^3 m^2)\right]$
Thermal Storage	$14.0 \cdot \left[\text{Storage size (MWh)}\right]$
Turbine	$520.3 \cdot \left[\text{Stage Size (MW)}\right]^{.8}$

was chosen as the second location because it has a high average insolation and thus acts as a limiting case for the system performance.

The sensitivity to restrictions on the amount of purchased energy was also investigated. The amount of fossil fuel and the amount of electricity which could be purchased were not restricted. However, the sum of the two quantities was restricted in the manner shown below.

$$NEP = \frac{(Q + E)}{(Q_c + E_c)}$$

Case	Restriction
1	$NEP < \infty$
2	$NEP \leq .55$
3	$NEP \leq .40$
4	$NEP \leq .25$
5	$NEP \leq .15$

Case 1 has no restriction on the amount of purchased energy, so the resulting system will simply be the most economic. Cases 2-5 correspond to increasing restrictions on the amount of energy which may be purchased. Solar energy will be required to make up the balance. The resulting system will be the most economical system subject to some constraint on the amount of energy which may be purchased.

Definition of the location and economic scenario is all that is required to initiate the LHS methodology. For each of the location/economic scenario combinations, 120 systems were randomly designed and their operation simulated. The results were used by the stepwise regression code to generate C, E and Q polynomials. Table III lists the nomenclature used to report the results and the general restrictions. Table IV contains the results of an LHS for the Nashville location with the four different economic scenarios listed in Table I. The restriction on the total installed electrical capacity can be seen at the top of the table. Since the amount of electricity and fossil fuel purchased to meet the application's needs are not dependent on the economics, only one E and one Q polynomial are listed. The r^2 values listed are for the classically defined correlation coefficient. In all cases, the values are quite high ($\geq$ 0.86) indicating a good correlation.

The E polynomial coefficients appear to be as expected. For example, this polynomial indicates electricity is needed to pump fluid through the collectors (the 15.20 X_c term) and the size of the turbine stages affects the amount of electricity purchased, with both stages having approximately the same effect.

TABLE III. Nomenclature and Restrictions on the Annualized Cost, Annual Fossil Fuel Purchase and Annual Electricity Purchase Polynomials

Nomenclature

C	-	annualized system cost (K$)
E	-	annual amount of electricity purchased (MWh)
Q	-	annual amount of fossil fuel purchased (MWh)
e_E	-	electricity cost inflation rate
e_Q	-	fossil fuel cost inflation rate
X_c	-	paraboloidal dish collector field size (10^3 m^2)
X_H	-	high pressure turbine stage size (MW)
X_L	-	low pressure turbine stage size (MW)
X_s	-	thermal storage size (MWh)

General Restrictions

$0 \le X_c \le 11.25$

$0 \le X_H \le .32$

$0 \le X_L \le .32$

$0 \le X_s \le 45.$

TABLE IV. C, E and Q Polynomials for Nashville

Restriction $\quad X_H + X_L \le .32 + .0123\ X_c$

$$E = 1536. + 15.20\ X_c - 5485.\ X_H - 5502.\ X_L + 3758.\ X_H^2 + 8022.\ X_H X_L + 3834.\ X_L^2 \qquad r^2 = .99$$

$$Q = 4269. - 501.6\ X_c + 17341.\ X_L + 28.28\ X_c^2 - 5.638\ X_c X_s - 1020.\ X_c X_H - 1145.\ X_c X_L + 117078.\ X_H^2 - 52668.\ X_H X_L + 89383.\ X_L^2 \qquad r^2 = .97$$

(Continued)

TABLE IV. C, E and Q Polynomials for Nashville (cont'd.)

$e_E = .10 \quad e_Q = .12$ Constant Electricity Cost

$$C = 146.3 + 7.979\ X_c - 294.4\ X_H + .3395\ X_c^2 - .08588\ X_cX_s - 8.905\ X_cX_H - 13.96\ X_cX_L + .01936\ X_s^2 + 1463.\ X_H^2 + 921.1\ X_L^2$$

$r^2 = .97$

$e_E = .14 \quad e_Q = .18$ Constant Electricity Cost

$$C = 255.9 + 1491.\ X_H^2 - 2162.\ X_HX_L + 2165.\ X_L^2 \quad r^2 = .86$$

$e_E = .10 \quad e_Q = .12$ Time-of-Day Electricity Cost

$$C = 147.3 + 5.020\ X_c - 151.7\ X_H + .3182\ X_c^2 - .07111\ X_cX_s + .01538\ X_s^2 + 1071.\ X_H^2 - 831.3\ X_HX_L + 880.9\ X_L^2$$

$r^2 = .97$

$e_E = .14 \quad e_Q = .18$ Time-of-Day Electricity Cost

$$C = 244.6 + 1579.\ X_H^2 - 2182.\ X_HX_L + 2205.\ X_L^2$$

$r^2 = .88$

The Q polynomial, on the other hand, contains a lot of information. As expected, it indicates solar collectors reduce the need for fossil fuel and the turbine stages increase the requirement. The high pressure stage can supply both high and low temperature process heat, while the low pressure turbine can supply only the low temperature demands. This significant difference is apparent in the Q polynomial. It shows, for example, that if a choice had to be made between having the high or low pressure stage, the better choice would be the high pressure stage, since much less fuel would be required for system operation.

The four equations for the annualized cost correspond to the four different economic scenarios. The first polynomial, for the case where the electricity cost inflation rate is 10% and the fossil fuel cost inflation rate is 12%, indicates that solar collectors increase the annualized cost of the system. The effect of storage is small, since its capital cost is relatively small and this cost is partially offset by its energy savings. The situation with the turbine stages is highly dependent on their sizes, with some cases reducing and others increasing the system's annualized cost.

The second annualized cost equation shows the high energy inflation rate case is near the breakeven point for the solar collectors and thermal storage. The first cost equation can be compared to the third to determine the effect of switching from a constant to a time-of-day electricity pricing schedule. This equation indicates that changing from one pricing schedule to another has little effect on system economics. The fourth cost equation again shows the solar collector field and thermal storage are near the breakeven point.

Table V contains some system designs for the Nashville location with the low energy inflation rates and five different restrictions on the amount of purchased energy. The "Analysis" column refers to the methodology used to arrive at the system design. The entry "LHS" indicates the design resulted from the polynomial search which yields an estimate on the polynomial's global optimum. The "MINA" entry refers to the methodology where the MINA routine is started at the polynomial's global optimum and eventually finds the optimum system design. The column titled "Energy Reduction" refers to the constraint placed on the total amount of purchased energy. C_c, E_c, and Q_c at the bottom of the page are the values for the conventional system.

TABLE V. System Designs for Nashville with the Standard Energy Inflation Rate and a Constant Price Schedule for Electricity

Analysis	Energy Reduction	X_c	X_s	X_H	X_L	C	E	Q
LHS	None	.03	7.03	.140	.003	135.9	831.	6573.
MINA	None	0.00	0.00	.115	.064	125.5	709.	5987.
LHS	45%	5.27	24.41	.052	.005	185.1	1318.	1769.
MINA	45%	4.03	14.94	.055	.005	165.9	1253.	1833.
LHS	60%	6.91	37.15	.082	.030	201.9	1078.	1146.
MINA	60%	5.78	31.77	.082	.033	182.8	1050.	1194.
LHS	75%	8.21	43.74	.082	.022	219.5	1136.	250.
MINA	75%	10.80	59.40	.114	.066	247.5	848.	555.
LHS	85%	NO SOLUTIONS FOUND						
MINA	85%	22.50	163.2	.197	.146	441.5	381.	455.

C_c = \$140.2 K E_c = 1447.2 MWh Q_c = 4166.4 MWh

The first set of designs has no restriction placed on it. The LHS solution indicates a fossil fuel fired total energy system is the optimum one and that is also the MINA result. The cost of this system is approximately 10% less than that of the conventional system and purchases about 20% more energy. If the turbine is operating at full power, it will exactly supply the maximum high temperature process heat demand. The requirement that the purchased energy be reduced by 45% causes both analyses to design STE systems with the emphasis being on supplying the process heat needs. This table indicates the polynomials' optima are near the surface's optima, as determined by MINA. For the 75% and 85% reduction cases, the maximum possible size for thermal storage was increased to allow MINA to design systems which meet the restrictions on purchased energy. The C, E, and Q polynomials were searched for a system which would reduce the total energy consumption by 85% but none was found within the previously discussed component size ranges. The MINA solution indicates that viable systems exist far outside this range and that they are very costly.

Much more information concerning the MINA system designs is available. This information includes:

1. Size and cost information on all dependent components
2. Amount of solar energy collected by each collector field.
3. Fraction of solar energy used immediately and the fraction routed through storage
4. Annual storage efficiency for all types
5. Fraction of the electrical demand supplied by the turbines, etc.

The results listed in Table V are plotted in Figures 8-10. In Figure 8 the normalized system cost is plotted versus the normalized energy purchase. The normalized cost is defined as the system's annualized cost divided by the conventional system's annualized cost ($140,200, in this case). The normalized energy purchase is defined in a similar manner; it is the system's total energy purchase (electrical plus fossil fuel) divided by that of the conventional system. This figure indicates that for moderate energy reductions (less than a 75% reduction) STES are not much more expensive than a conventional system. This is a very significant result, especially when the near-term beginning year of operation (1982) is considered. However, when solar energy is required to greatly reduce the

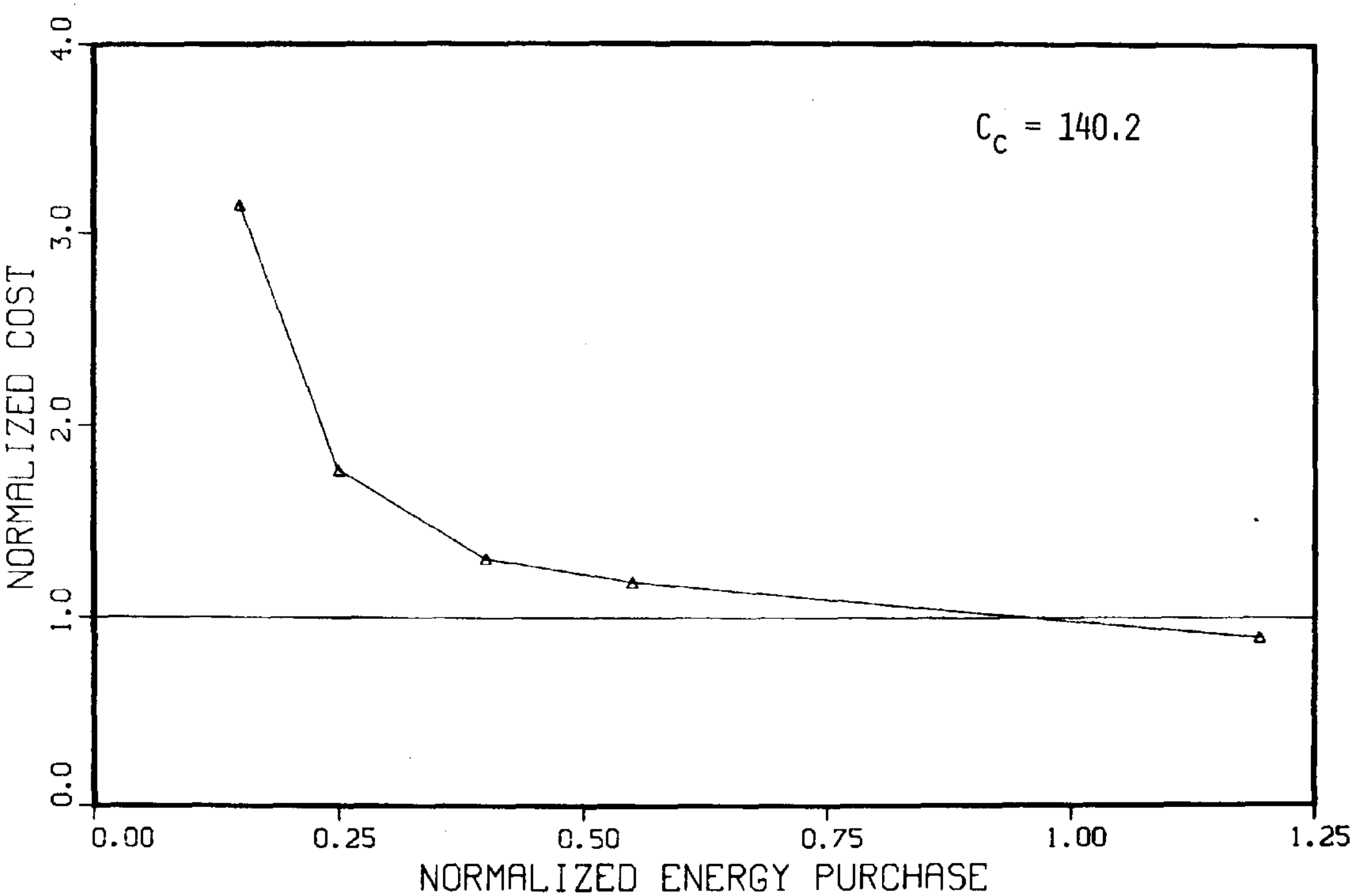

Figure 8. Results for the Nashville Location with the Standard Inflation Rate and the Constant Pricing Schedule for Electricity.

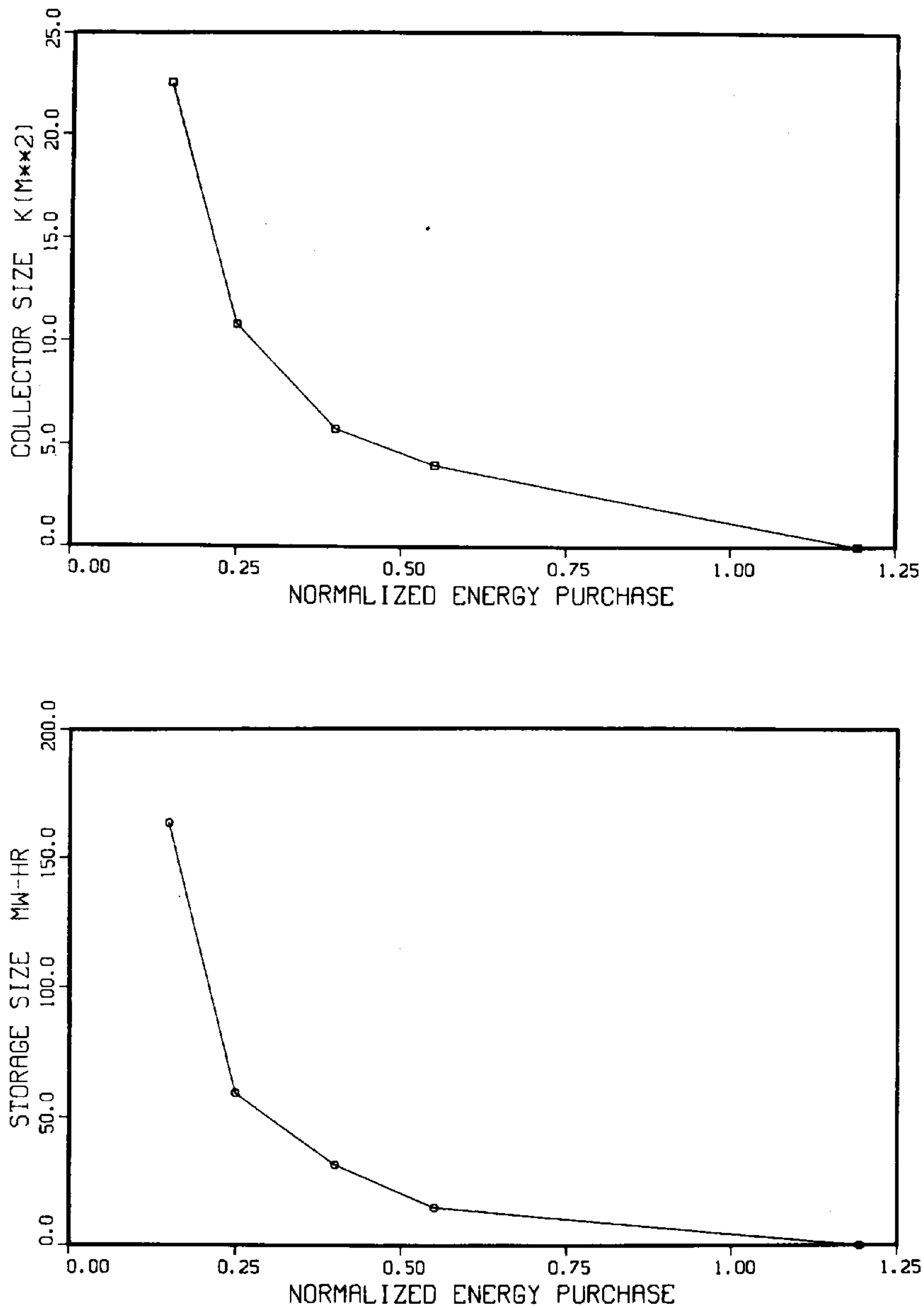

Figure 9. Results for the Nashville Location with the Standard Inflation Rate and the Constant Pricing Schedule for Electricity.

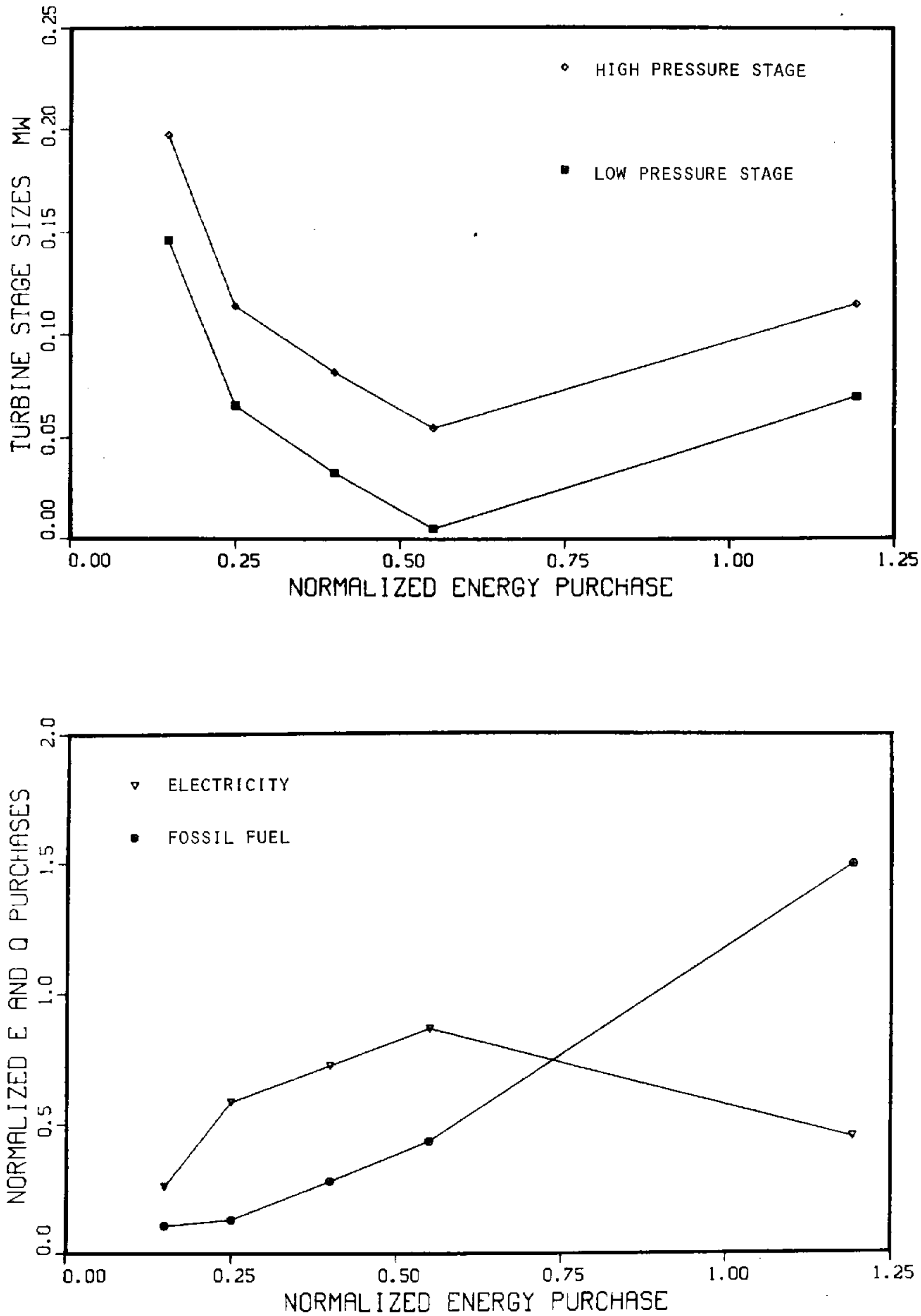

Figure 10. Results for the Nashville Location with the Standard Inflation Rate and the Constant Pricing Schedule for Electricity.

system energy purchases, the annualized cost becomes quite high; in this case more than three times higher than a conventional system's cost when energy purchases are reduced by 85%. The least expensive system is a fossil fuel total energy system which has an annualized cost slightly less than a conventional system and purchases more conventional energy.

Figures 9 and 10 show the changes in collector field size, storage size, and turbine stage sizes as the amount of energy purchased is varied. These figures show a general trend of increasing size with increasing restrictions on purchased energy. The turbine curves in Figure 10 have a large value for a large normalized energy purchase because a fossil fuel total energy system is the optimum system when there is no restriction on purchased energy.

The bottom plot of Figure 10 shows the variation in the purchase of electricity and in fossil fuel as the restriction on the total energy purchase is changed. The electricity purchase and the fossil fuel purchase values are normalized by dividing them respectively by the conventional system's purchased amount of electricity (1447.2 MWh) and fossil fuel (4166.4 MWh). The fossil fuel total energy system purchases large amounts of fossil fuel to produce electricity and provide thermal energy. Figure 10 indicates this system purchases 50% more fossil fuel than a conventional system, reducing the amount of electricity purchased by about 50%. For the STES a general trend of decreasing purchases of both electricity and fossil fuel with increasing restrictions on the total amount of purchased energy is observed. The electricity curve is beginning to level out at low values of total purchased energy because the turbine is not operated during the weekend when about 5% of the electricity is consumed.

Figures 11-13 show the effect of increasing the energy cost inflation rate. Previously, it had been observed that the high inflation rate was near the breakeven point for solar collectors and thermal storage. These figures indicate that collectors and storage can reduce the annualized cost. In this case, the optimum system has an annualized cost that is about 90% that of a conventional system with a small collector field, thermal storage and a turbine. The effect of the collectors and storage on the annualized cost is, as the cost polynomial indicates, slight. If, for example, the size of the collector field is halved, the cost increases by 2%, from $225,700 to $229,900. If, instead, the size of the storage is reduced from 11.7 MWh to 1.17 MWh, the cost increases by 5%. In both cases the lost solar energy was replaced by fossil fuel which has about the same annualized cost as the component whose size was reduced.

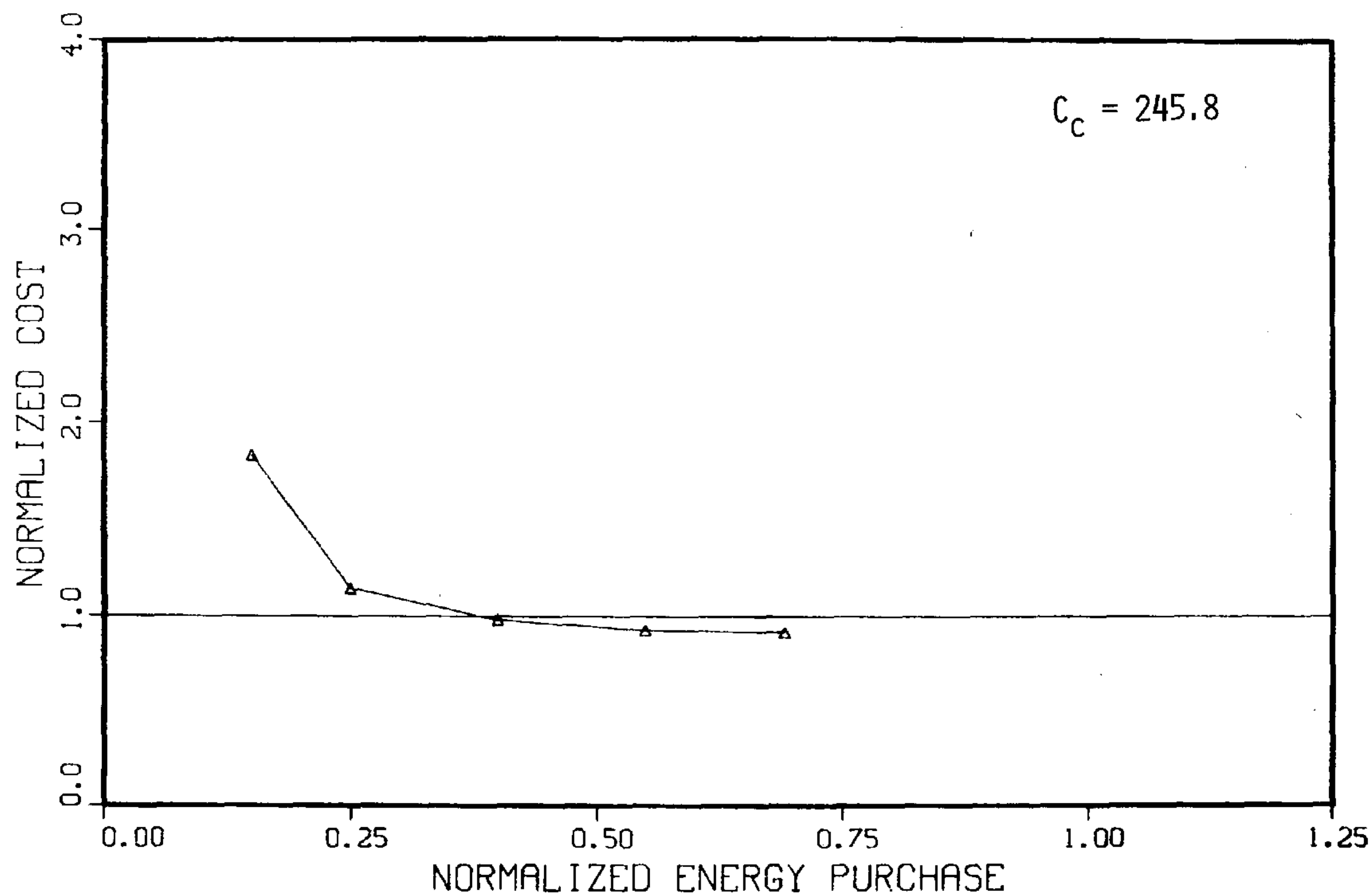

Figure 11. Results for the Nashville Location with the High Inflation Rate and the Constant Pricing Schedule for Electricity.

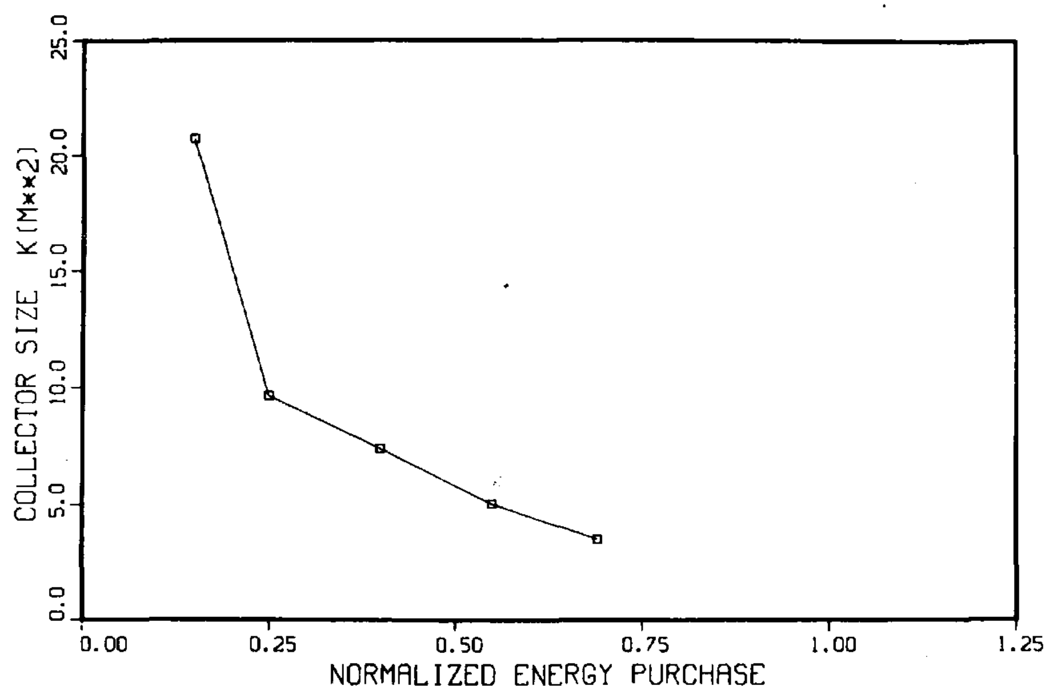

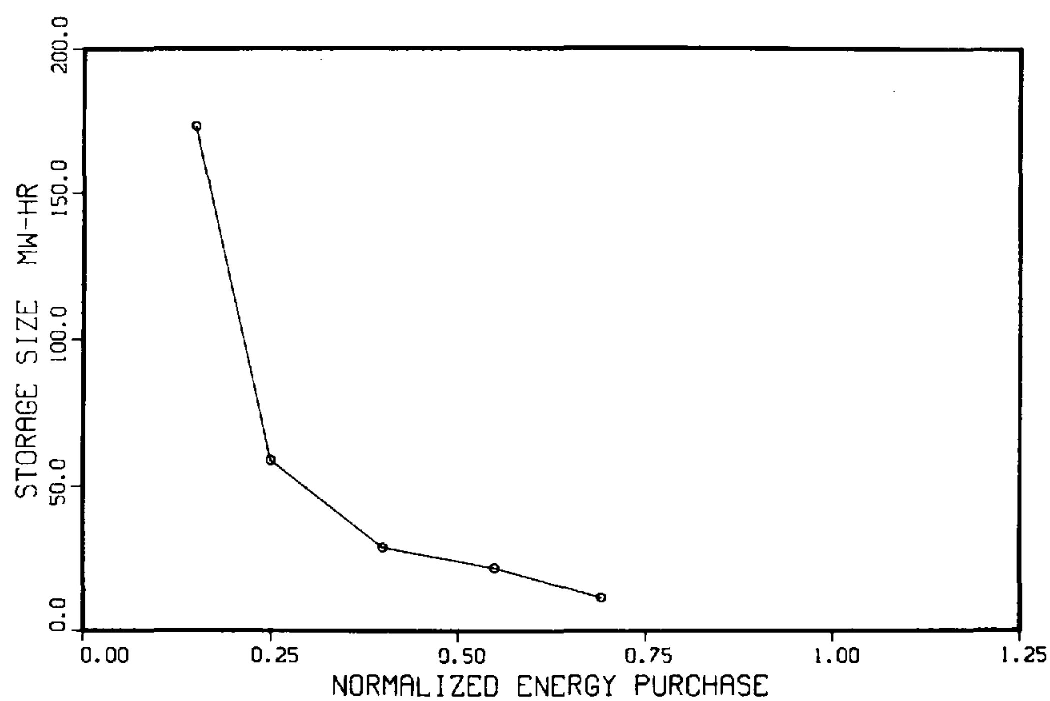

Figure 12. Results for the Nashville Location with the High Inflation Rate and the Constant Pricing Schedule for Electricity.

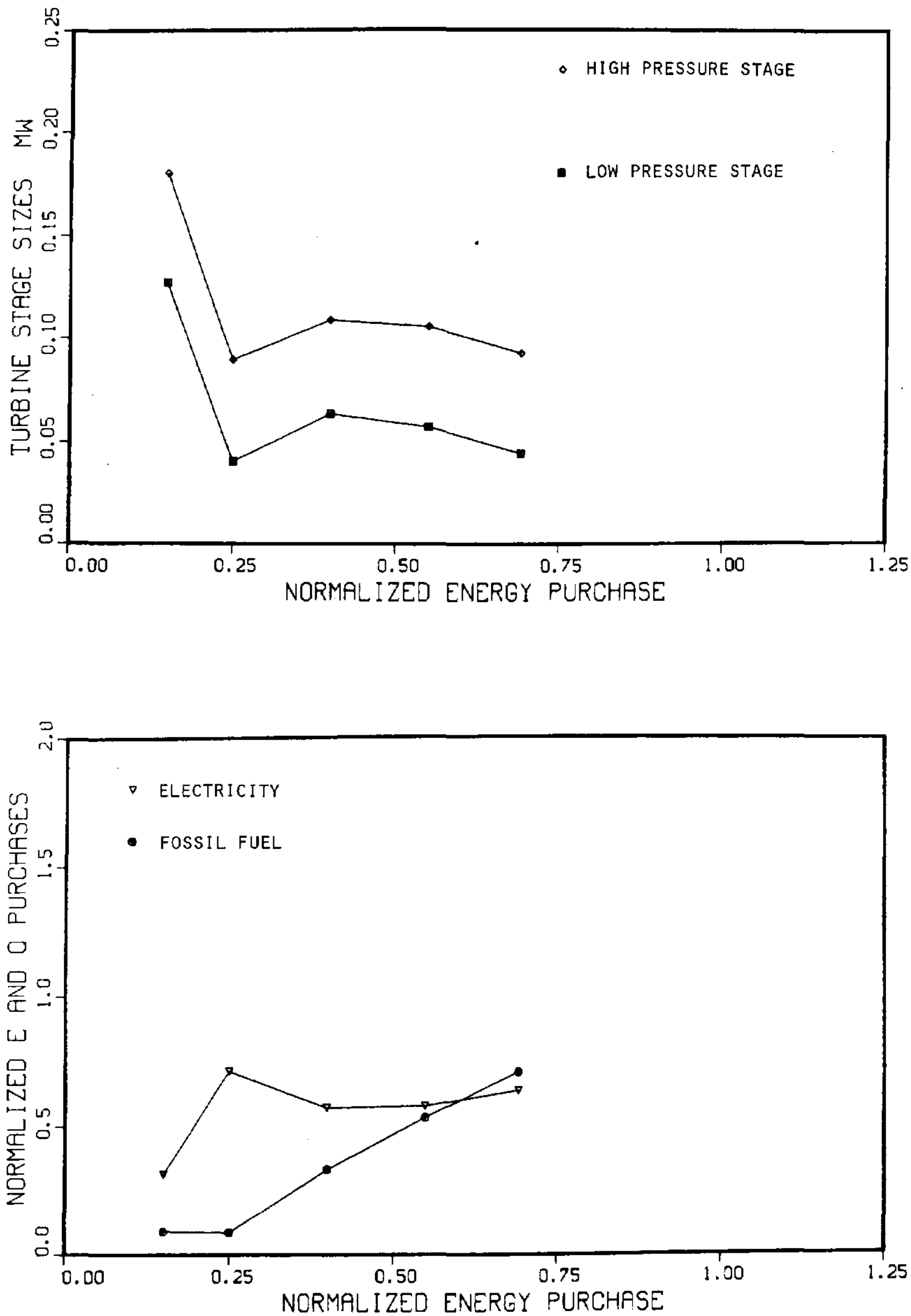

Figure 13. Results for the Nashville Location with the High Inflation Rate and the Constant Pricing Schedule for Electricity.

Figures 14-19 show the effect of time-of-day pricing. Comparison of Figures 14-16 with the constant pricing counterparts in Figures 8-10 shows only one significant difference; the time-of-day pricing system chooses larger turbine stages for the 40% normalized energy purchased case and so purchases less electricity than its constant pricing counterpart. This seems reasonable, since much of the turbine operation occurs during the portion of the day when time-of-day price schedule electricity cost is relatively high. Comparison of Figures 11-13 with the Figures 17-19 counterparts, indicates that time-of-day pricing schedule has little effect on system design when the inflation rates are high. It should be noted that slight changes in the time-of-day pricing schedule may have a major impact on system design; these results should not be generalized.

Table VI lists the C, E, and Q polynomials for a system in Albuquerque. Figure 20 shows the paraboloidal dish collector output profiles based upon the Nashville and Albuquerque TMY data. The dotted line indicates the average collector output. Figure 20 indicates a dish collector in Albuquerque will collect approximately twice as much energy in a year as one in Nashville. Comparison of the Nashville and Albuquerque Q polynomials shows that the dish collector in Albuquerque collects about twice as much energy as one in Nashville. This result also shows up on the E polynomial, where it can be seen that a collector requires twice as much electricity for operation in Albuquerque.

The C polynomials are also strongly affected by the higher insolation. For example, the Nashville polynomial for the high inflation, constant electricity cost case indicates the collectors and storage have little effect on the system's annualized cost, while in Albuquerque the C polynomial indicates collectors and storage will reduce the system's cost. Since the collectors have a substantial effect on the cost, terms like $X_c X_s$ and $X_c X_H$ become important and therefore are present in this cost polynomial.

Figures 21-32 show the Albuquerque system designs for the four different economic scenarios with purchased energy restrictions in each case. Solar collectors are more economical in Albuquerque than in Nashville, but it is shown in Figure 22 that they are not included in the unconstrained optimum system (a fossil fuel total energy system). Further investigation of Figure 21 shows that only the most restrictive STE

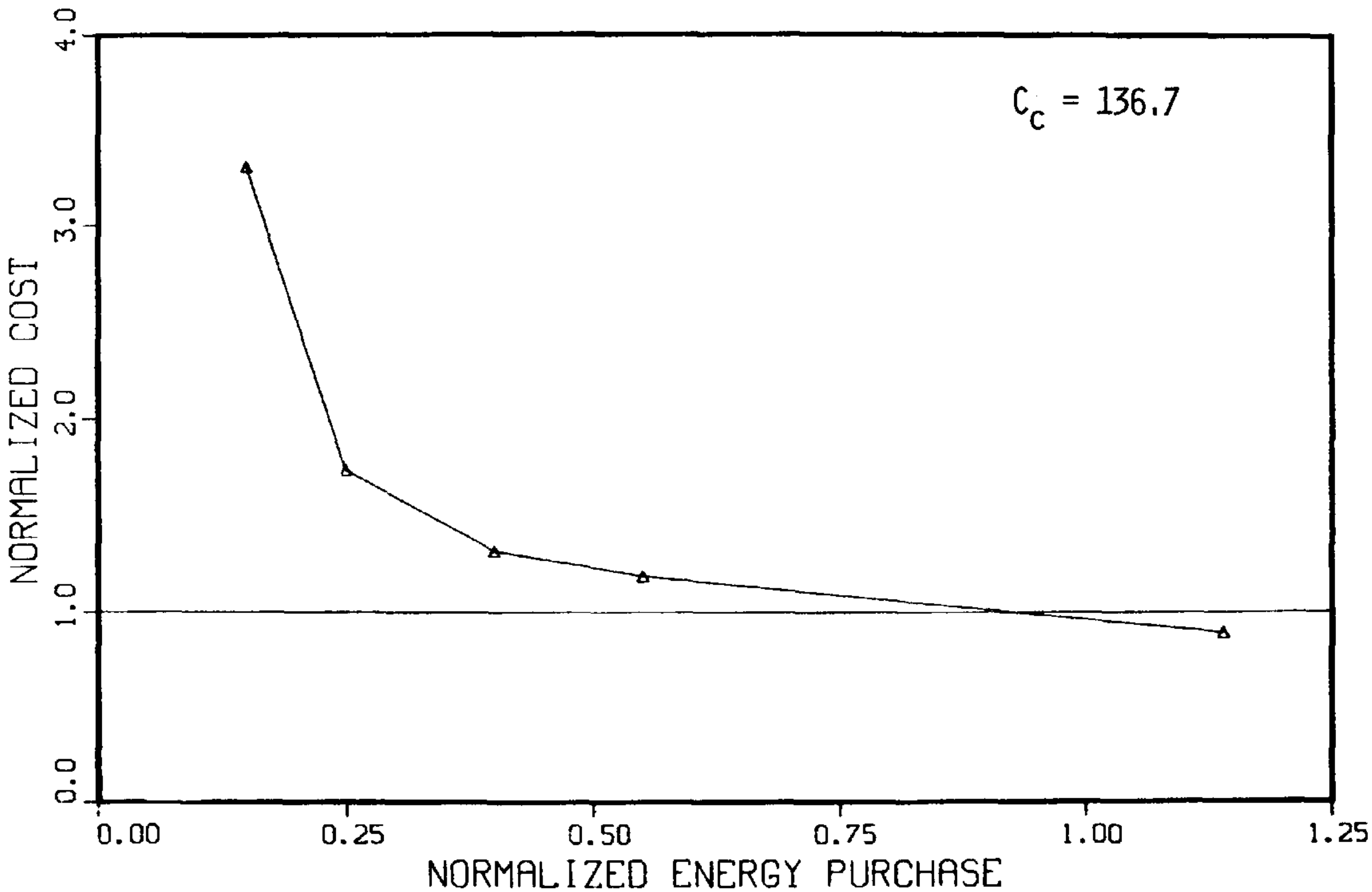

Figure 14. Results for the Nashville Location with the Standard Inflation Rate and the Time-of-Day Pricing Schedule for Electricity.

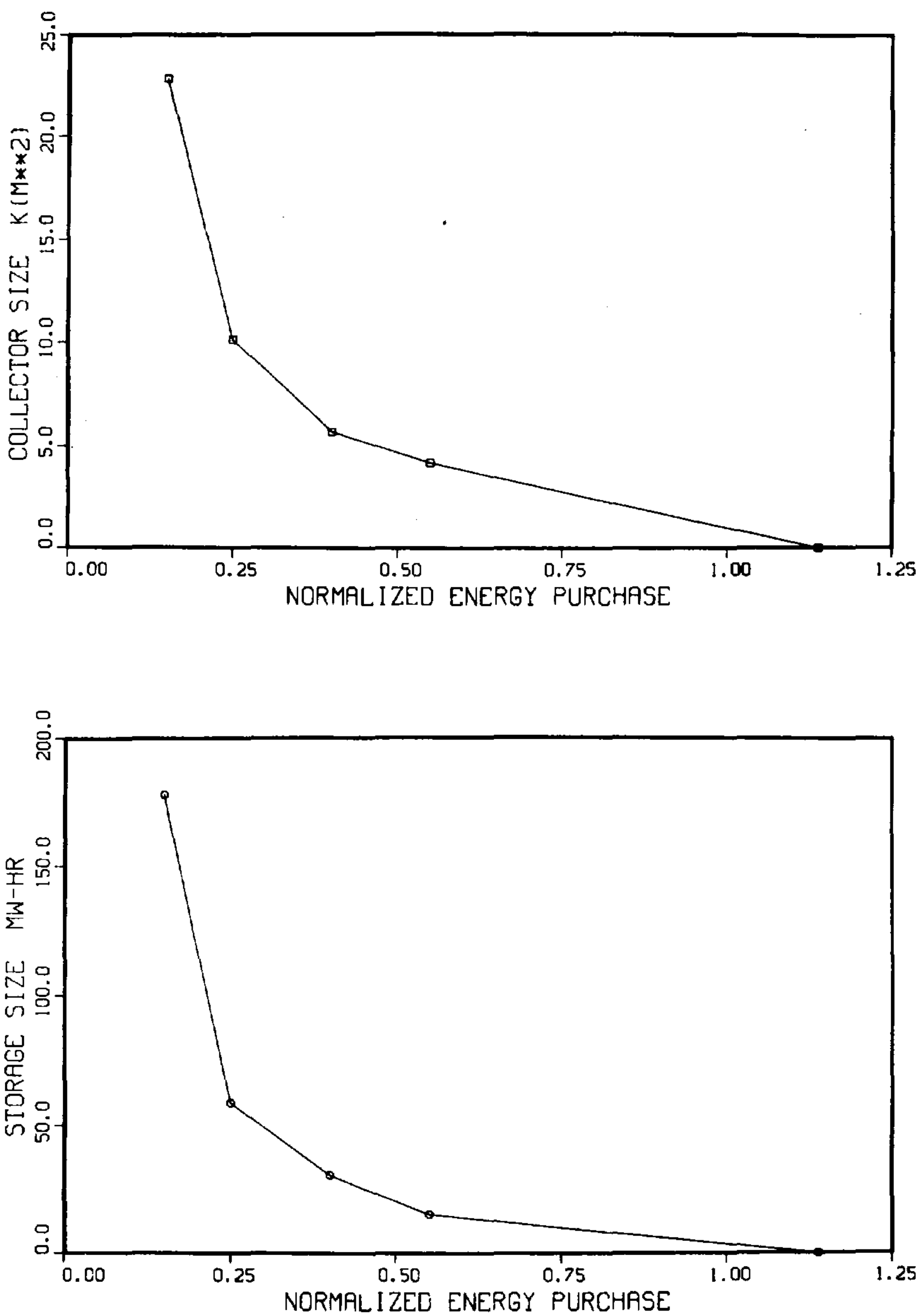

Figure 15. Results for the Nashville Location with the Standard Inflation Rate and the Time-of-Day Pricing Schedule for Electricity.

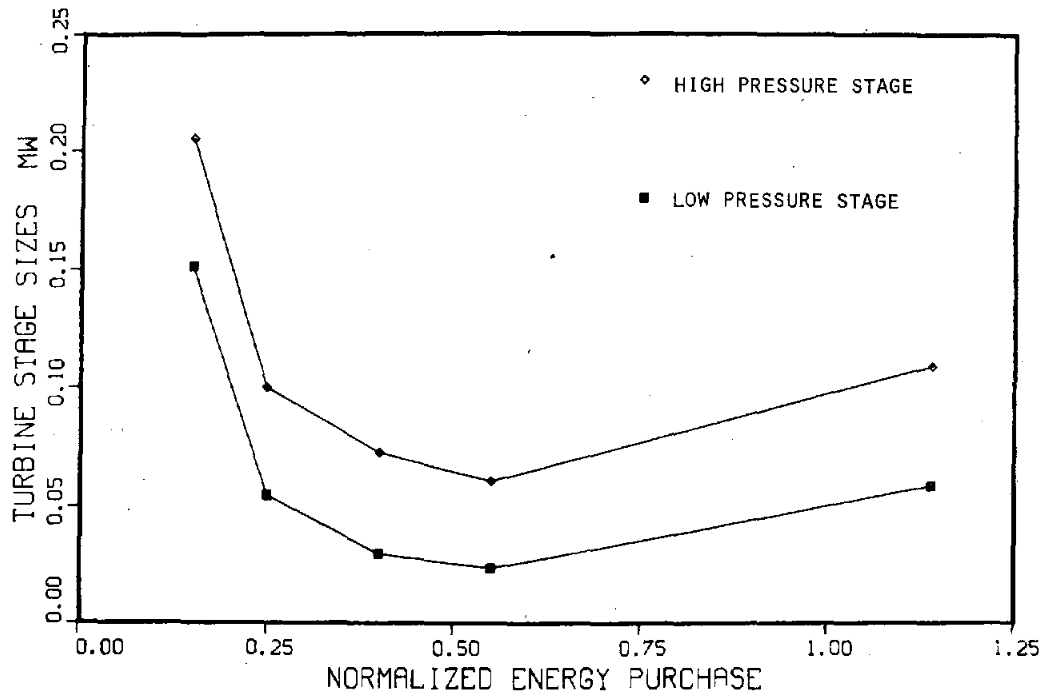

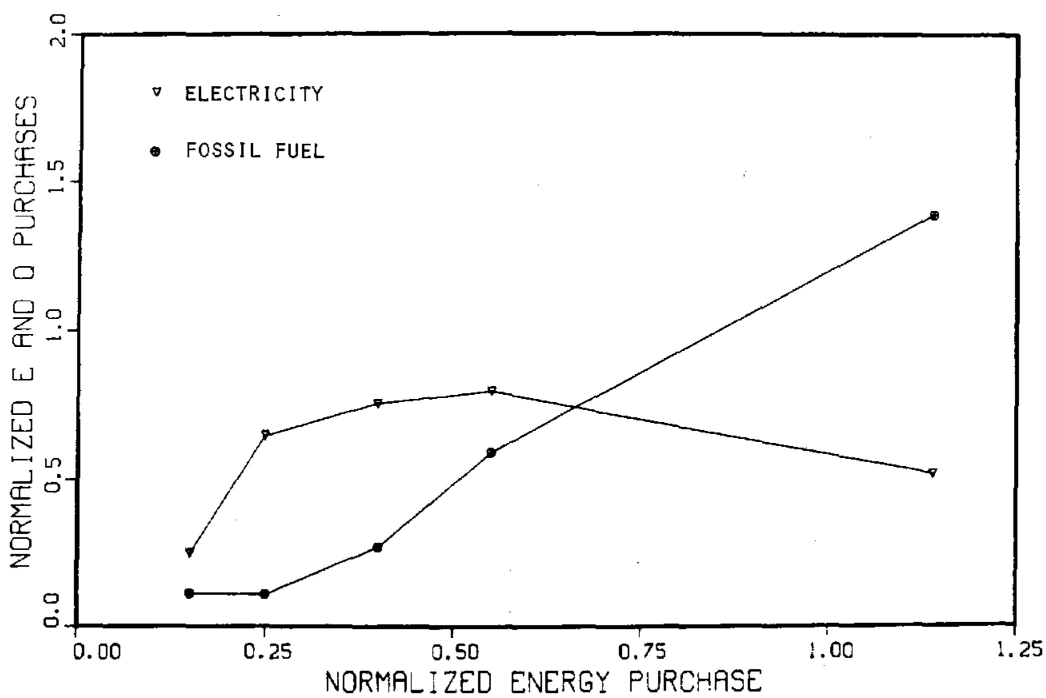

Figure 16. Results for the Nashville Location with the Standard Inflation Rate and the Time-of-Day Pricing Schedule for Electricity.

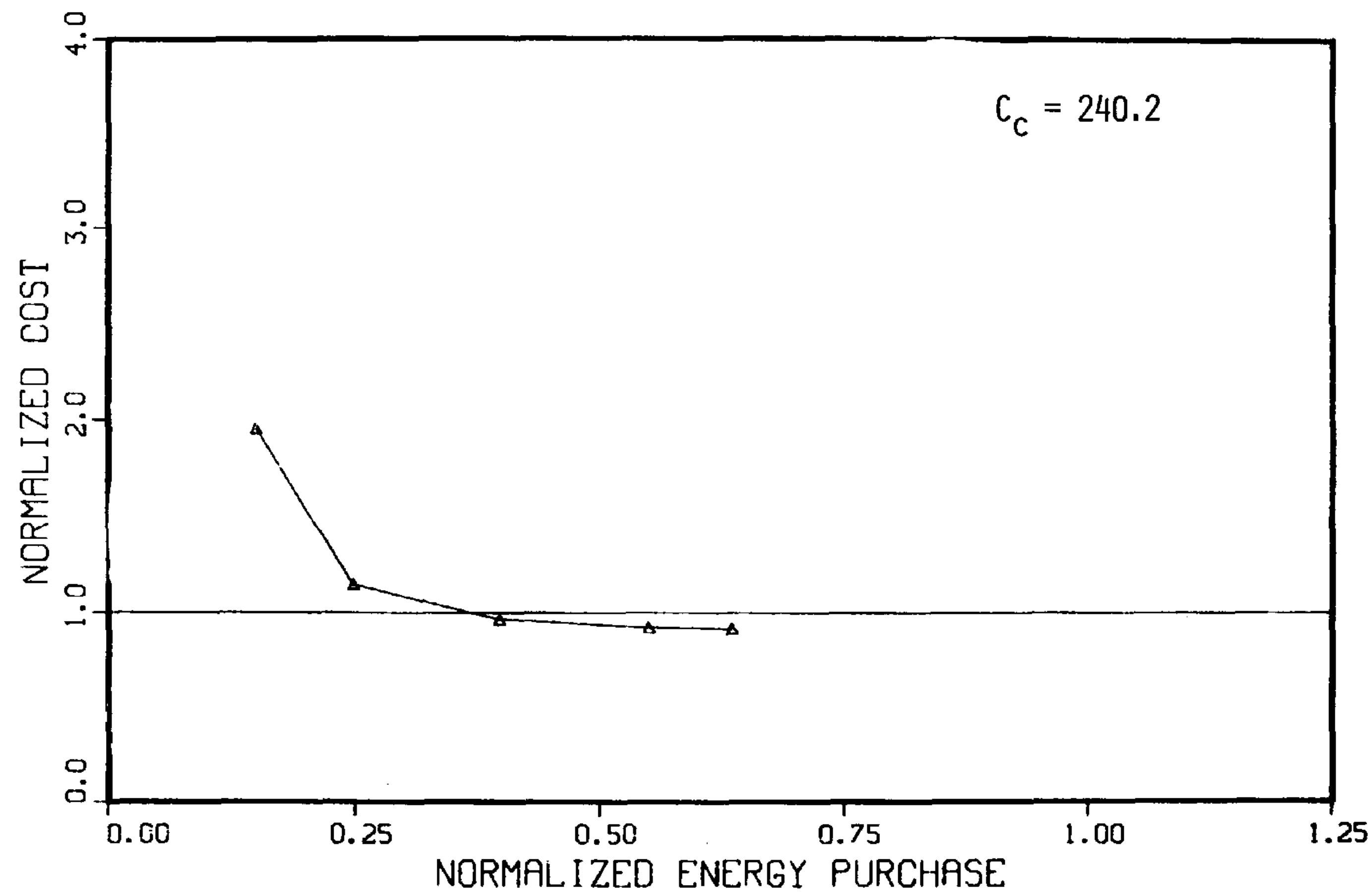

Figure 17. Results for the Nashville Location with the High Inflation Rate and the Time-of-Day Pricing Schedule for Electricity.

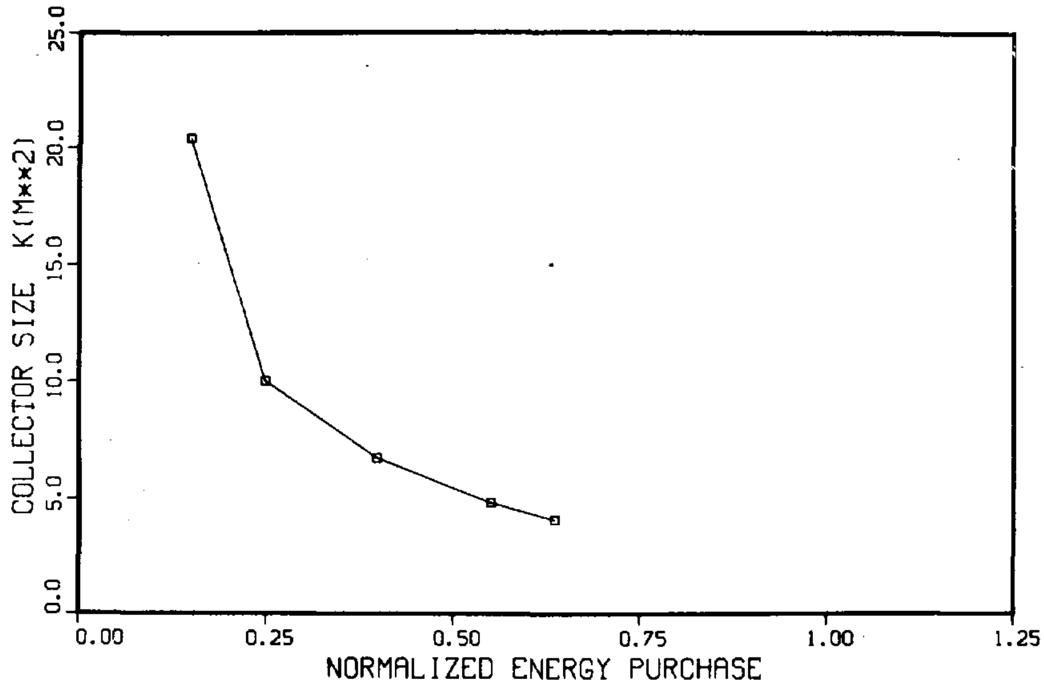

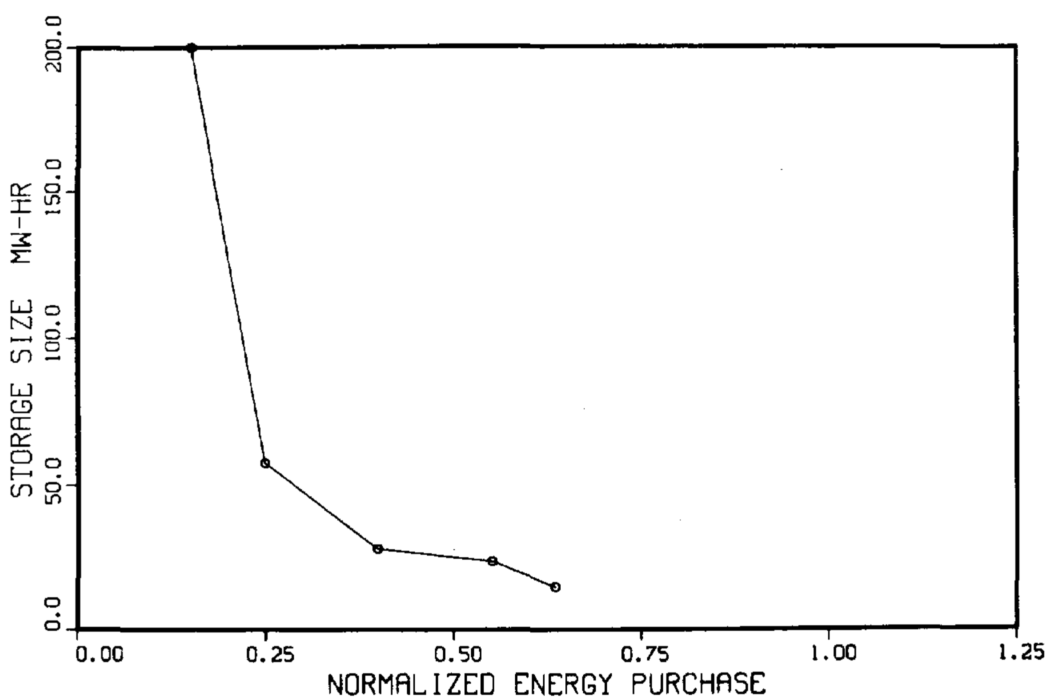

Figure 18. Results for the Nashville Location with the High Inflation Rate and the Time-of-Day Pricing Schedule for Electricity.

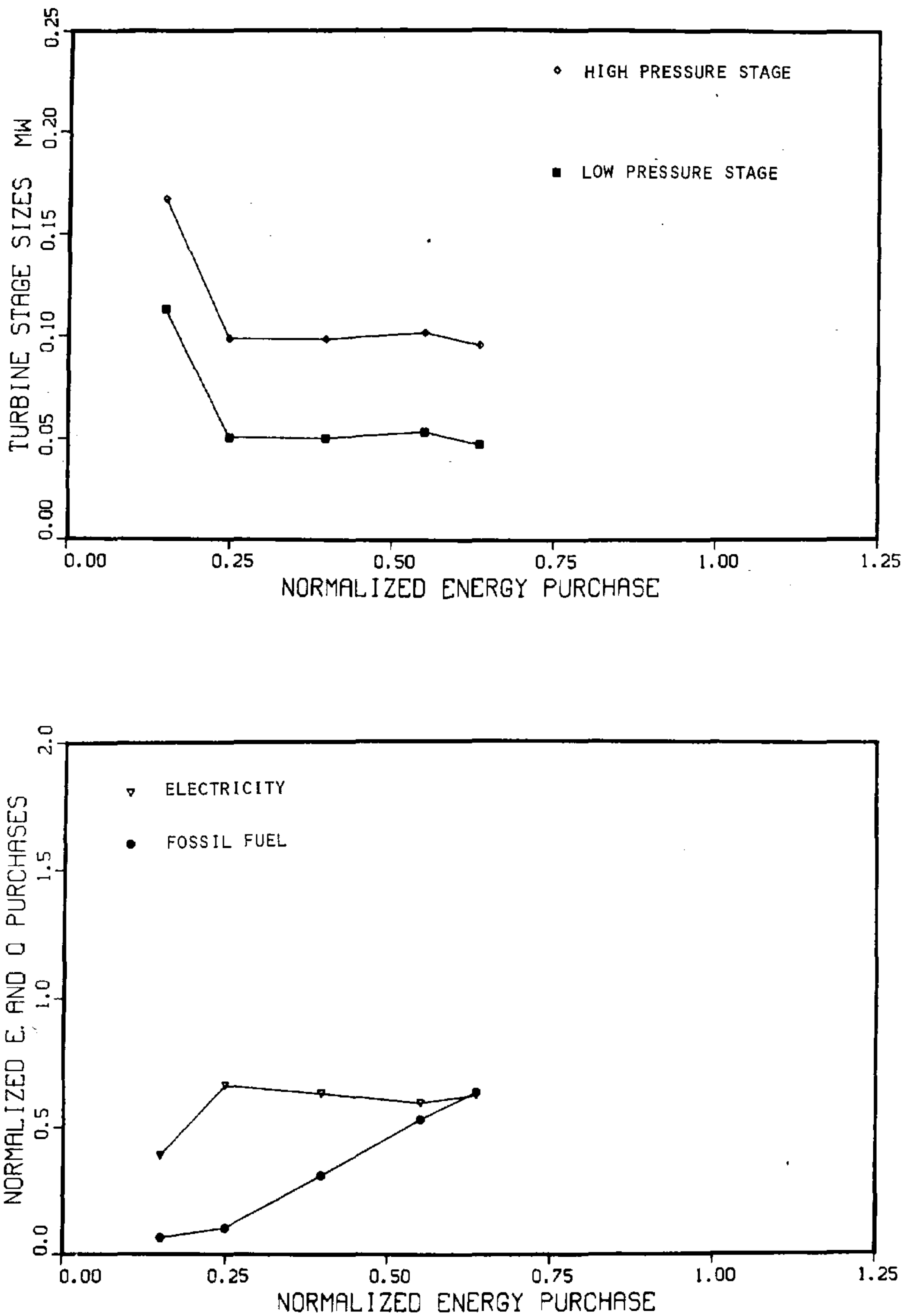

Figure 19. Results for the Nashville Location with the High Inflation Rate and the Time-of-Day Pricing Schedule for Electricity.

TABLE VI. C, E, and Q Polynomials for Albuquerque

Restriction $\quad X_H + X_L \leq .32 + .0131\ X_c$

$$E = 1510. + 31.24\ X_c - 5124.\ X_H - 5049.\ X_L + 2704.\ X_H^2 + 5754.\ X_H X_L + 2616.\ X_L^2 \qquad r^2 = 1.00$$

$$Q = 4436. - 1150.\ X_c + 14165.\ X_L + 109.8\ X_c^2 - 8.915\ X_c X_s - 2149.\ X_c X_H - 3024.\ X_c X_L + 95769.\ X_H^2 + 88422.\ X_L^2 \qquad r^2 = .94$$

$e_E = .10 \quad e_Q = .12$ Constant Electricity Cost

$$C = 135.2 + 1.269\ X_c^2 - .07875\ X_c X_s - 23.58\ X_c X_H - 28.70\ X_c X_L + .01613\ X_s^2 + 613.9\ X_H^2 - 518.6\ X_H X_L + 985.9\ X_L^2 \qquad r^2 = .93$$

$e_E = .14 \quad e_Q = .18$ Constant Electricity Cost

$$C = 246.3 - 11.31\ X_c - 1.527\ X_s^2 + 2.332\ X_c^2 - .1794\ X_c X_s - 49.33\ X_c X_H - 62.61\ X_c X_L + .05708\ X_s^2 - 3.700\ X_s X_H + 1693.\ X_H^2 - 668.0\ X_H X_L + 2173.\ X_L^2 \qquad r^2 = .88$$

$e_E = .10 \quad e_Q = .12$ Time-of-Day Electricity Cost

$$C = 154.6 - 3.563\ X_c - 140.6\ X_H + 1.462\ X_c^2 - 23.20\ X_c X_H - 32.78\ X_c X_L + 905.4\ X_H^2 + 872.3\ X_L^2 \qquad r^2 = .89$$

$e_E = .14 \quad e_Q = .18$ Time-of-Day Electricity Cost

$$C = 248.3 - 12.83\ X_c - 1.667\ X_s + 2.728\ X_c^2 - .2225\ X_c X_s - 51.77\ X_c X_H - 77.61\ X_c X_L + .05097\ X_s^2 + 1159.\ X_H^2 + 2264.\ X_L^2 \qquad r^2 = .85$$

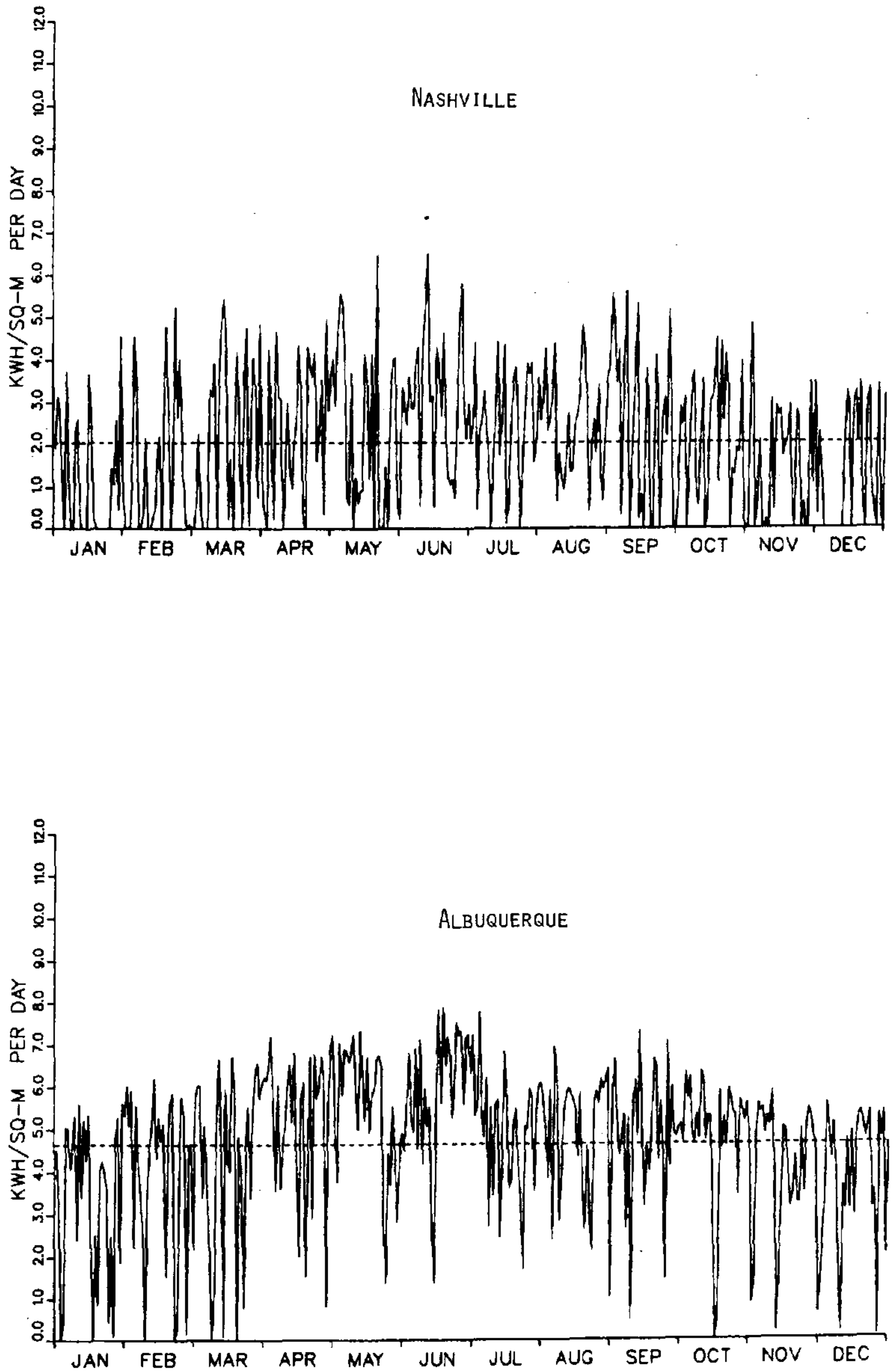

Figure 20. Collector Output Profiles

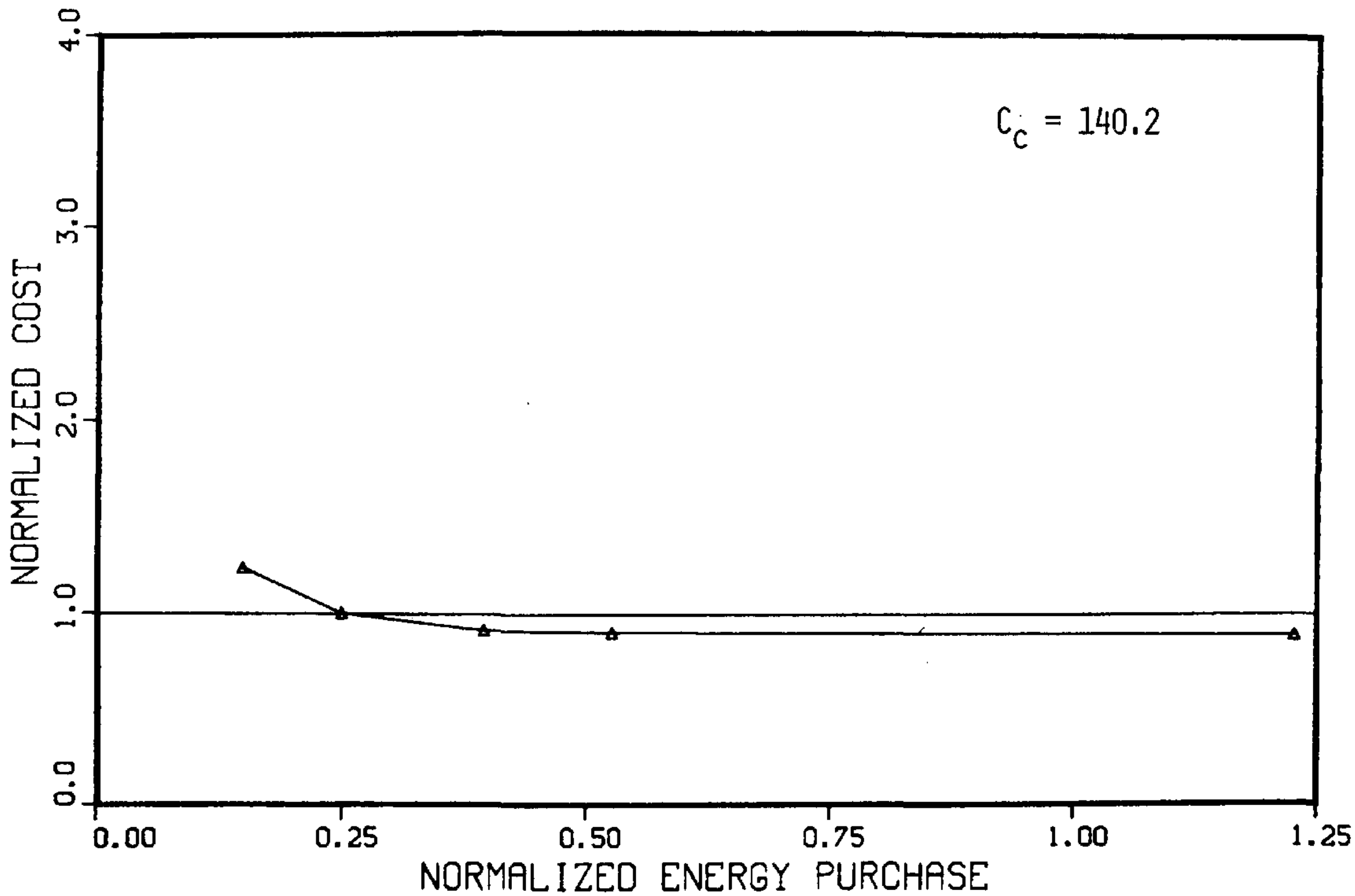

Figure 21. Results for the Albuquerque Location with the Standard Inflation Rate and the Constant Price Schedule for Electricity.

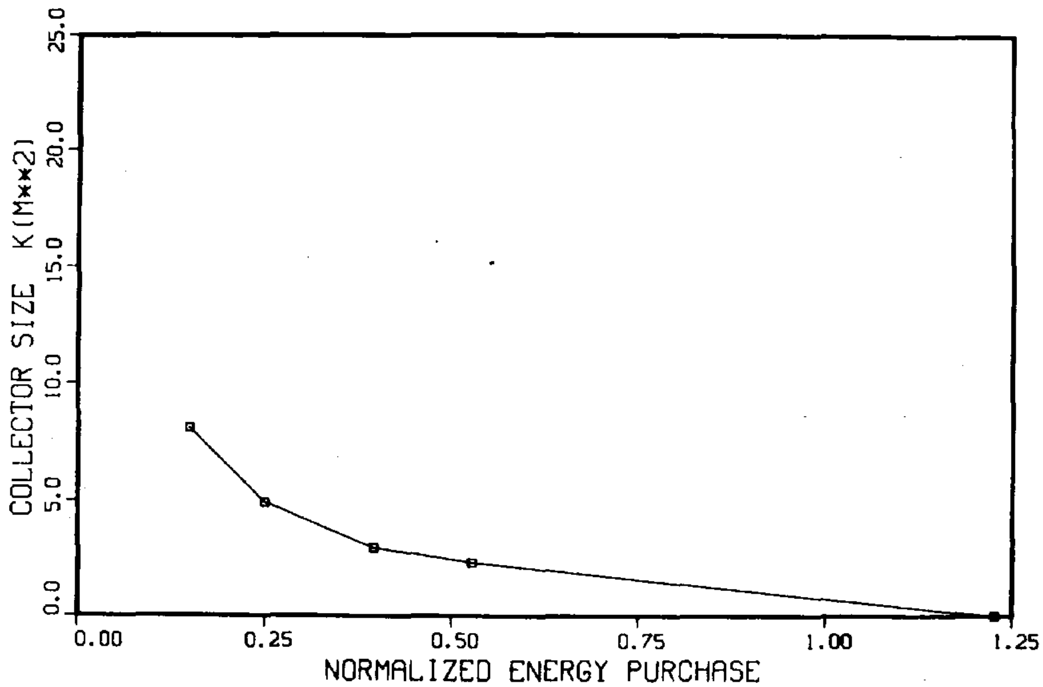

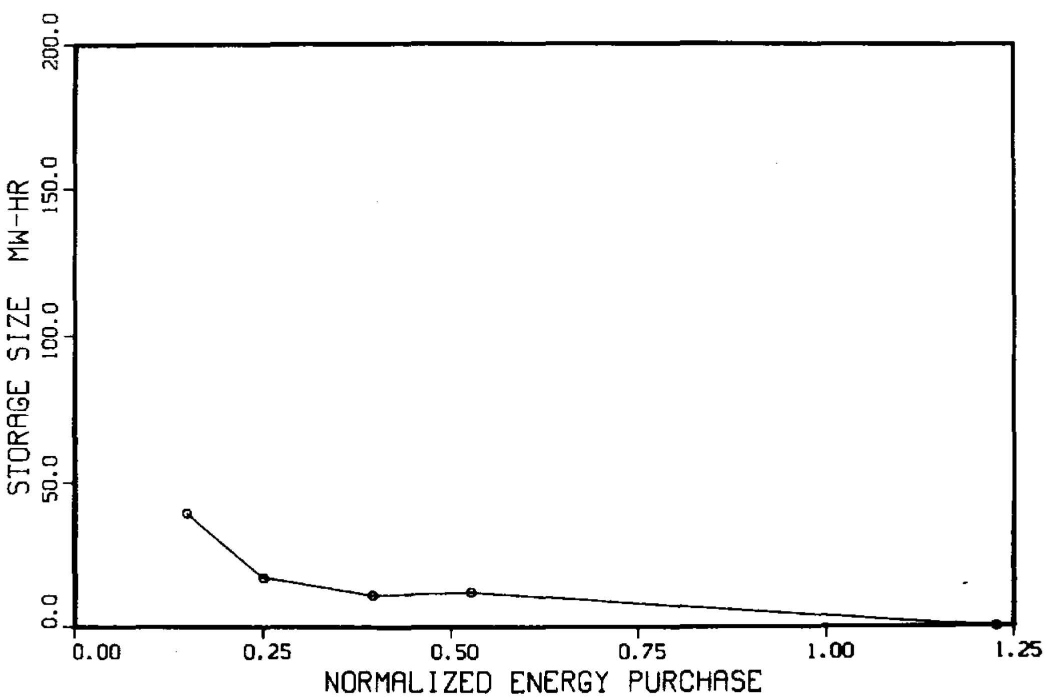

Figure 22. Results for the Albuquerque Location with the Standard Inflation Rate and the Constant Price Schedule for Electricity.

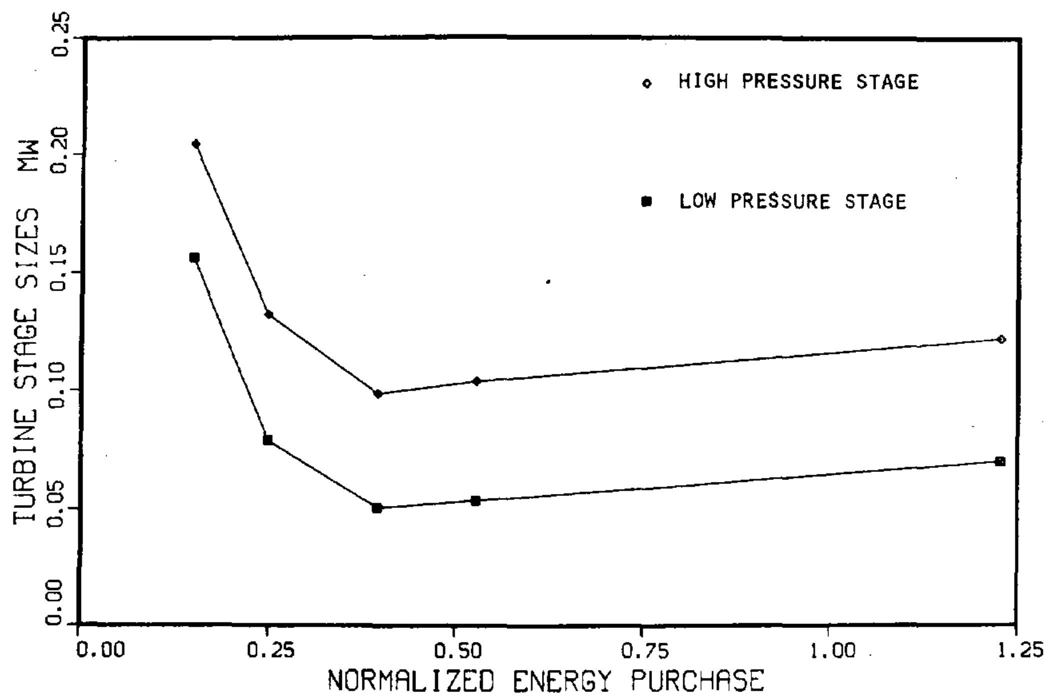

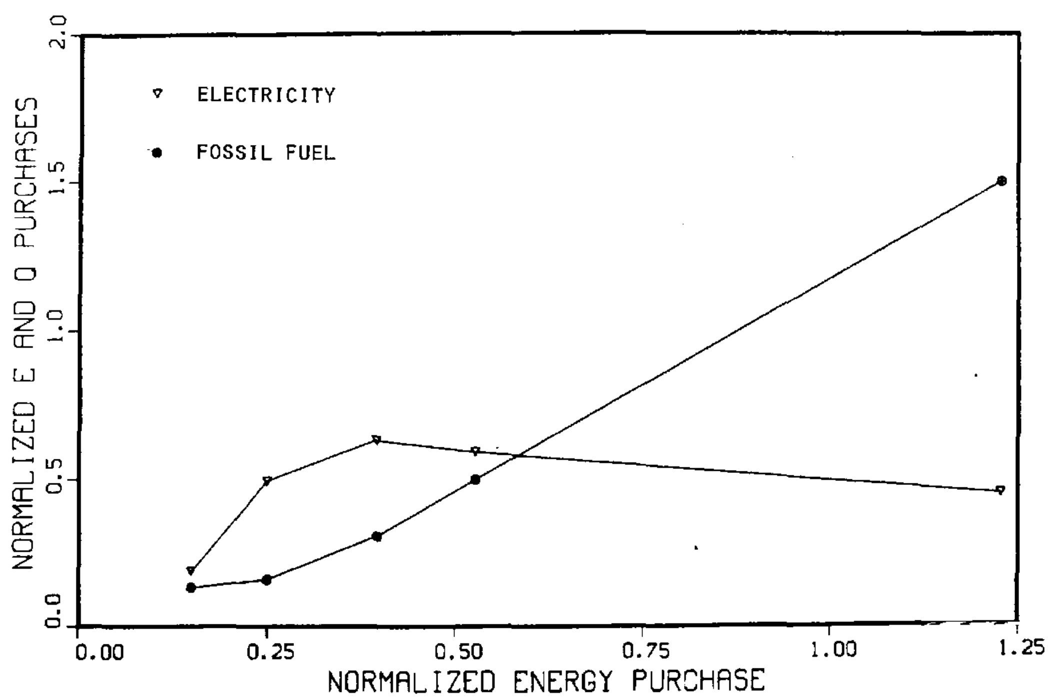

Figure 23. Results for the Albuquerque Location with the Standard Inflation Rate and the Constant Price Schedule for Electricity.

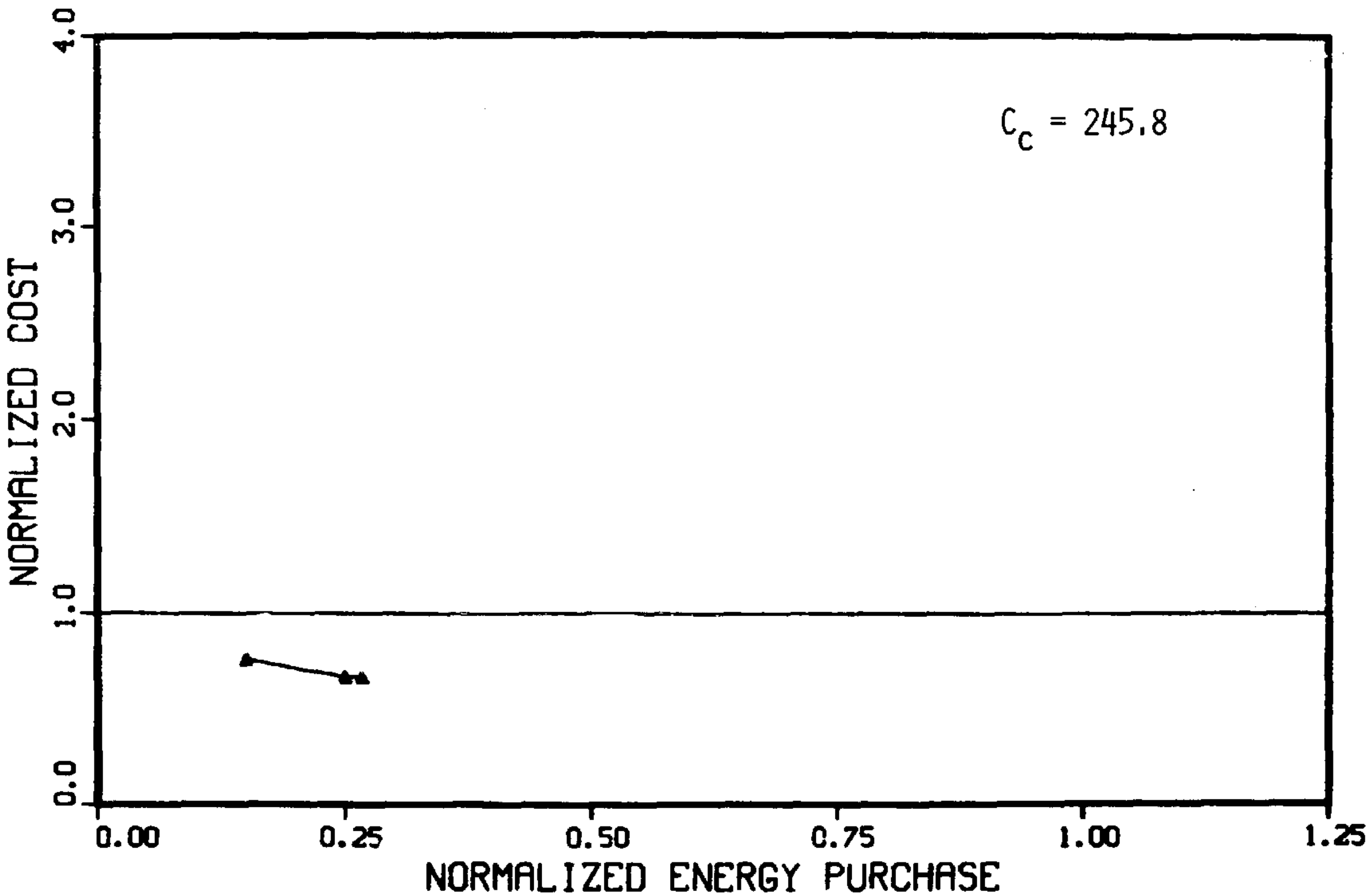

Figure 24. Results for the Albuquerque Location with the High Inflation Rate and the Constant Pricing Schedule for Electricity.

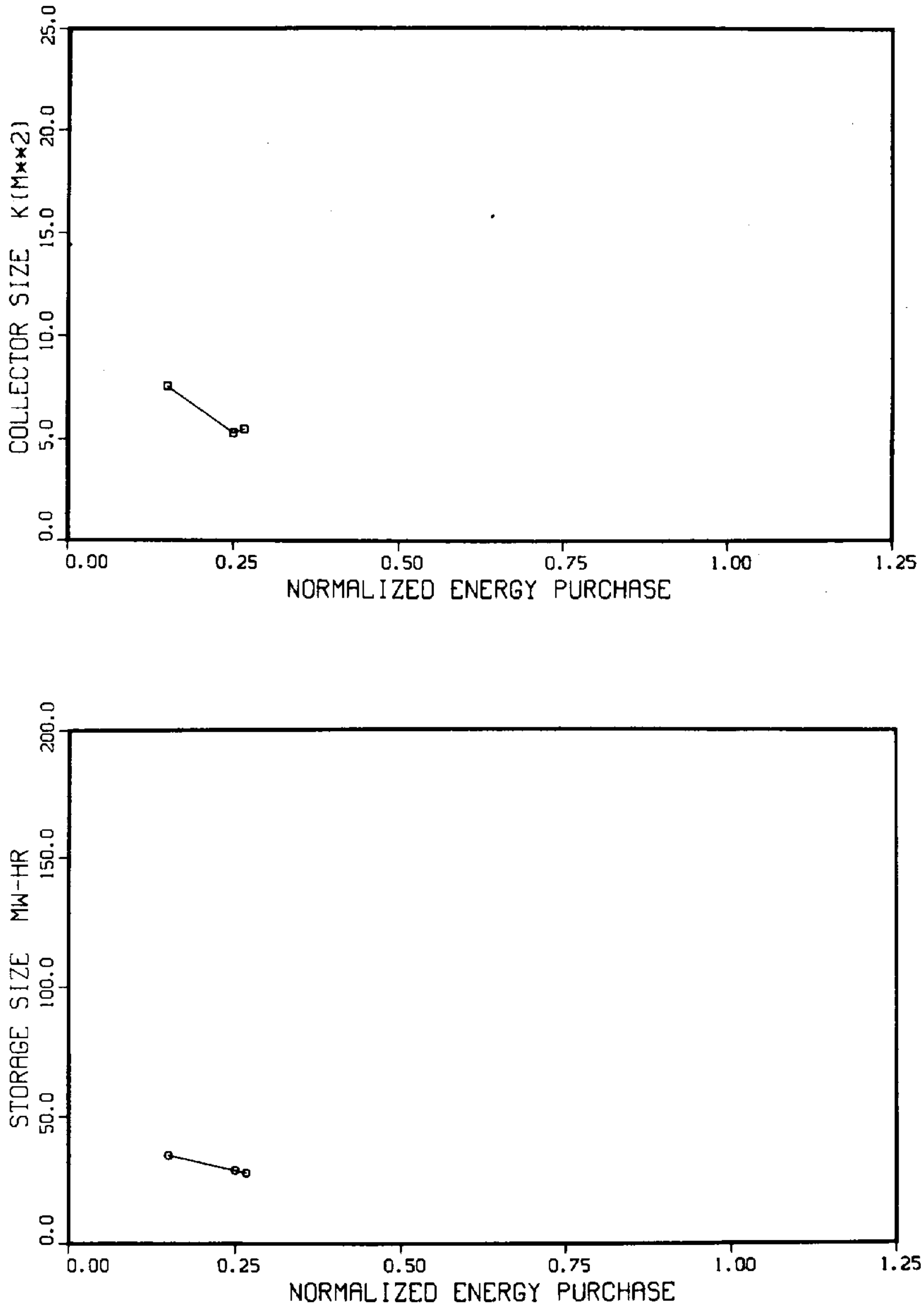

Figure 25. Results for the Albuquerque Location with the High Inflation Rate and the Constant Pricing Schedule for Electricity.

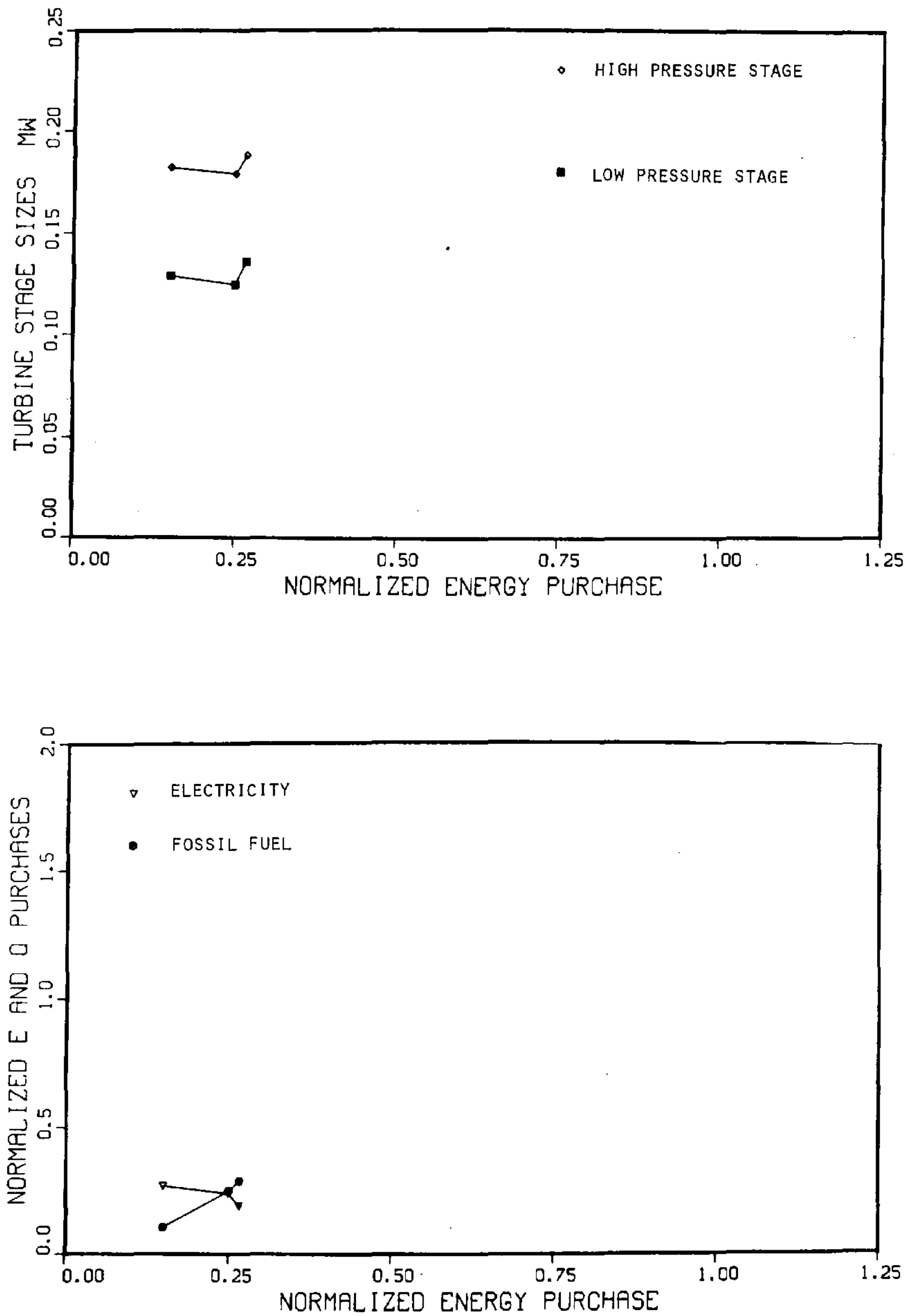

Figure 26. Results for the Albuquerque Location with the High Inflation Rate and the Constant Pricing Schedule for Electricity.

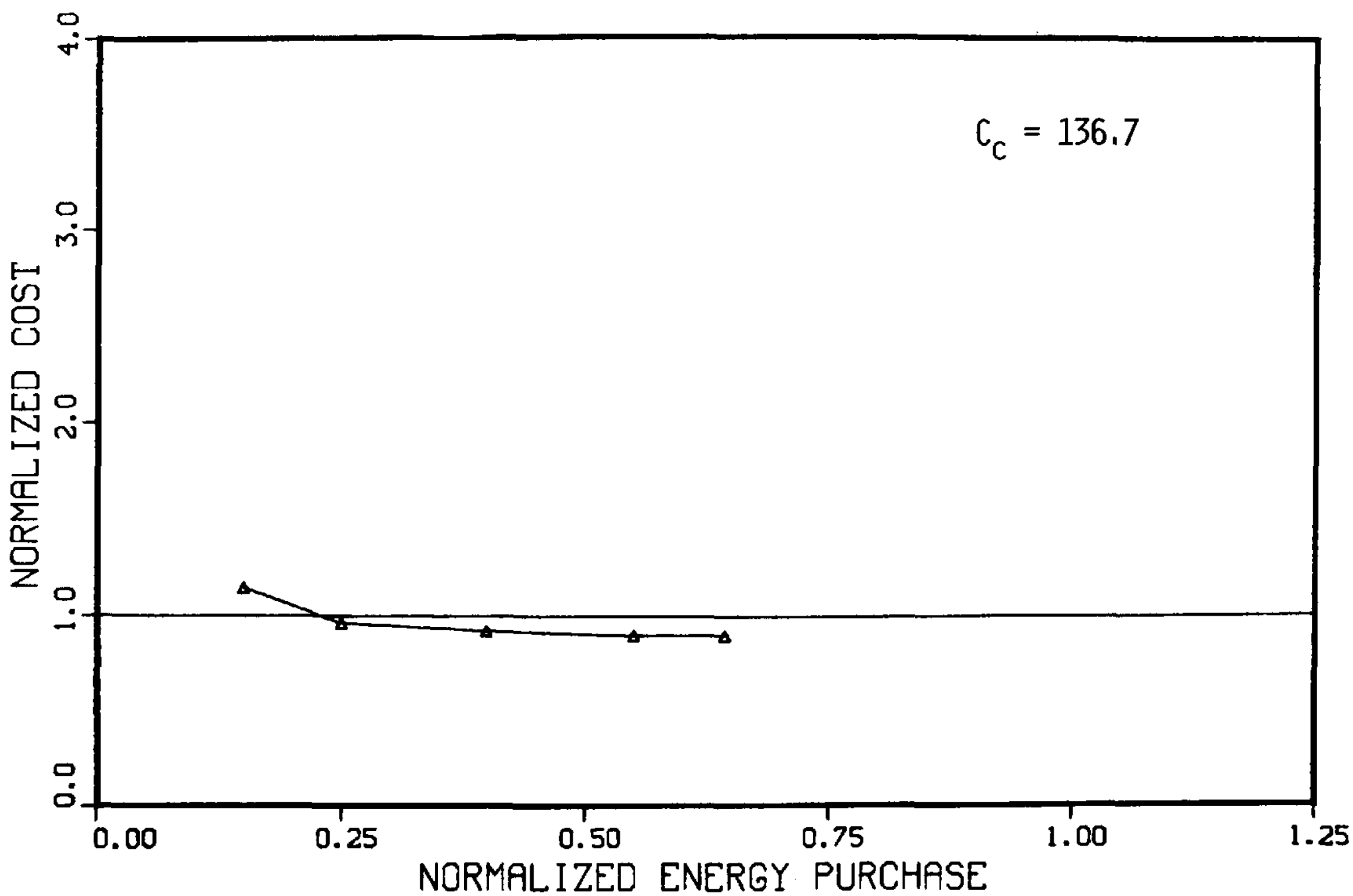

Figure 27. Results for the Albuquerque Location with the Standard Inflation Rate and a Time-of-Day Price Schedule for Electricity.

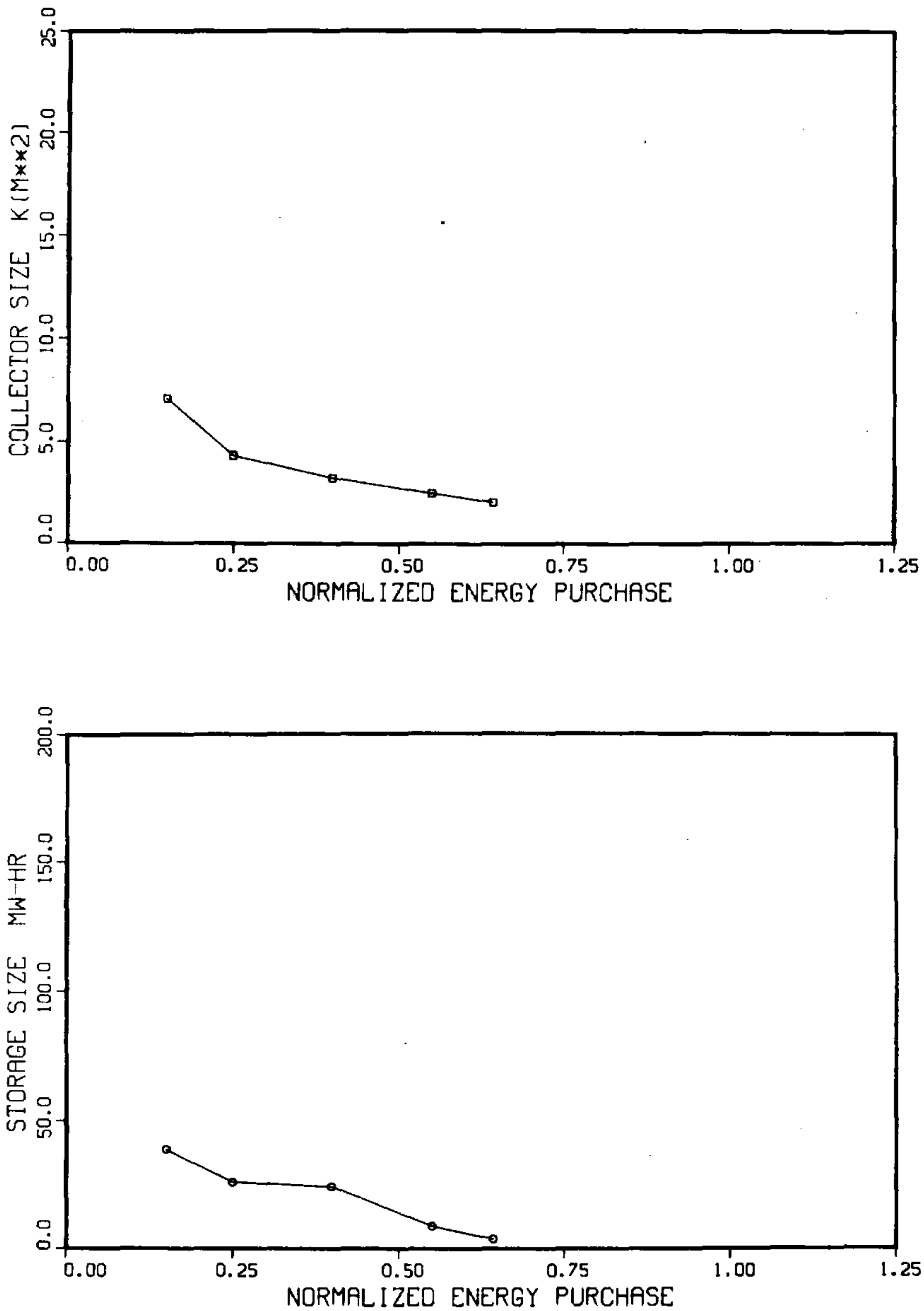

Figure 28. Results for the Albuquerque Location with the Standard Inflation Rate and a Time-of-Day Price Schedule for Electricity.

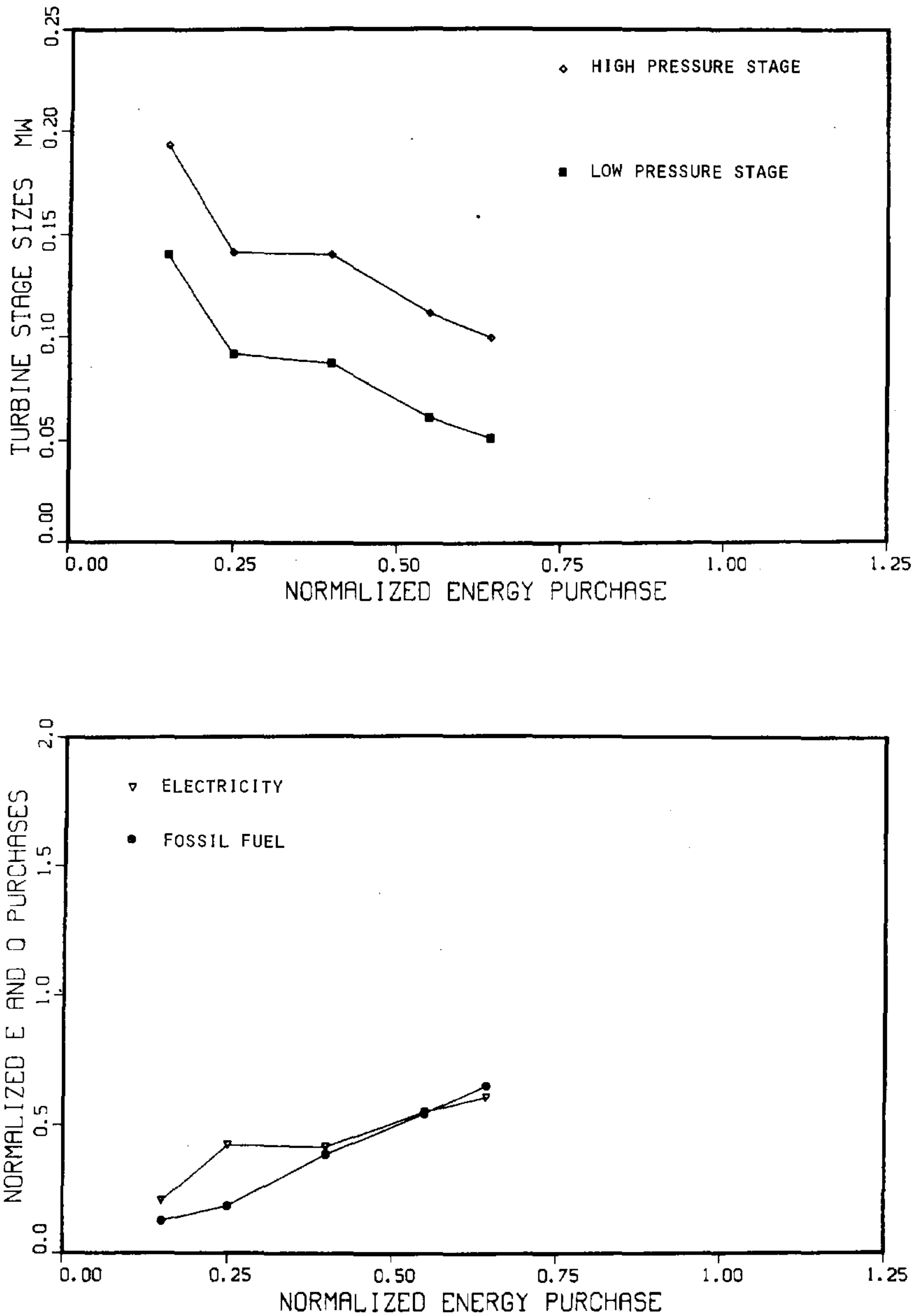

Figure 29. Results for the Albuquerque Location with the Standard Inflation Rate and a Time-of-Day Price Schedule for Electricity.

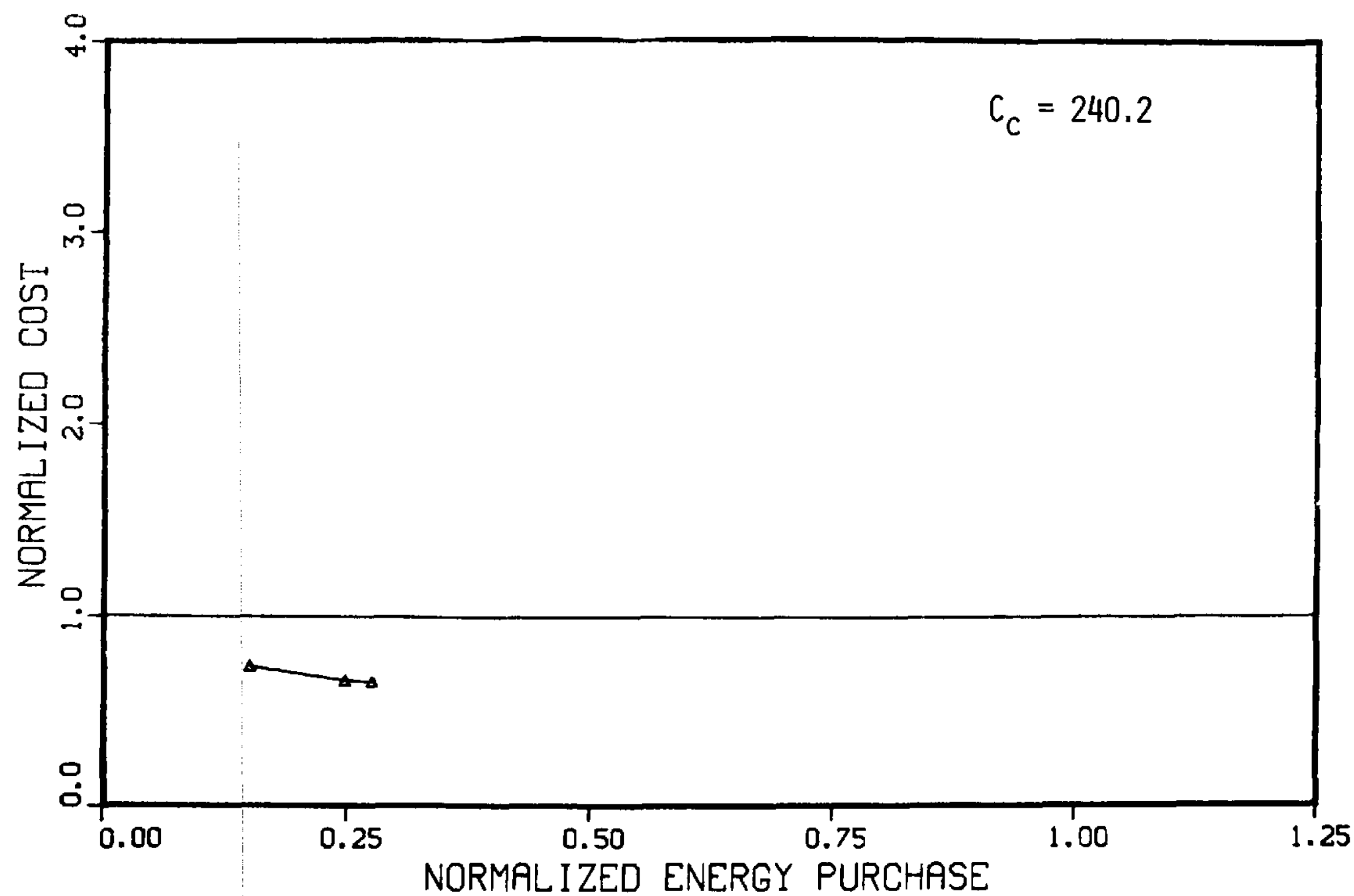

Figure 30. Results for the Albuquerque Location with the High Inflation Rate and the Time-of-Day Price Schedule for Electricity.

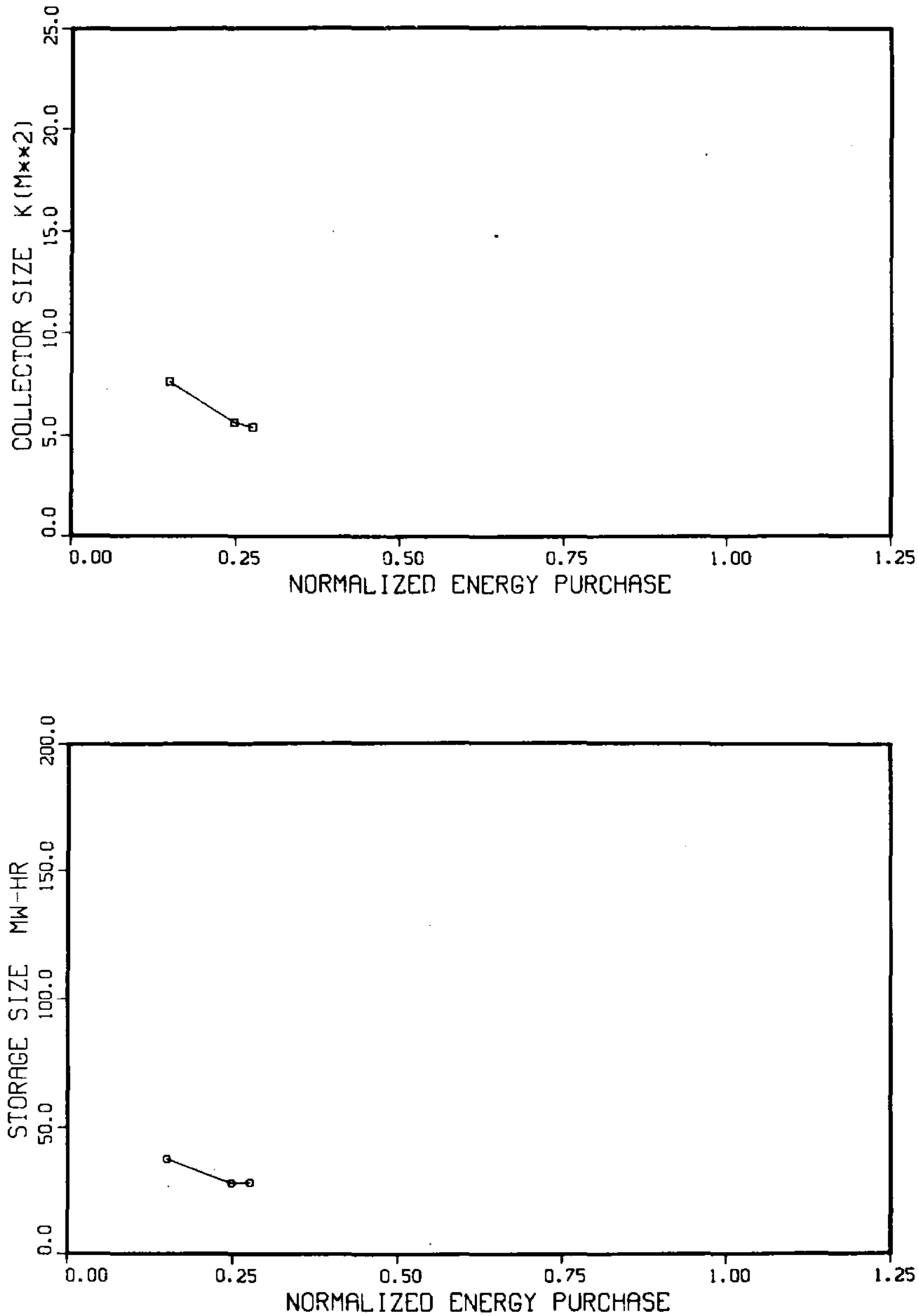

Figure 31. Results for the Albuquerque Location with the High Inflation Rate and the Time-of-Day Price Schedule for Electricity.

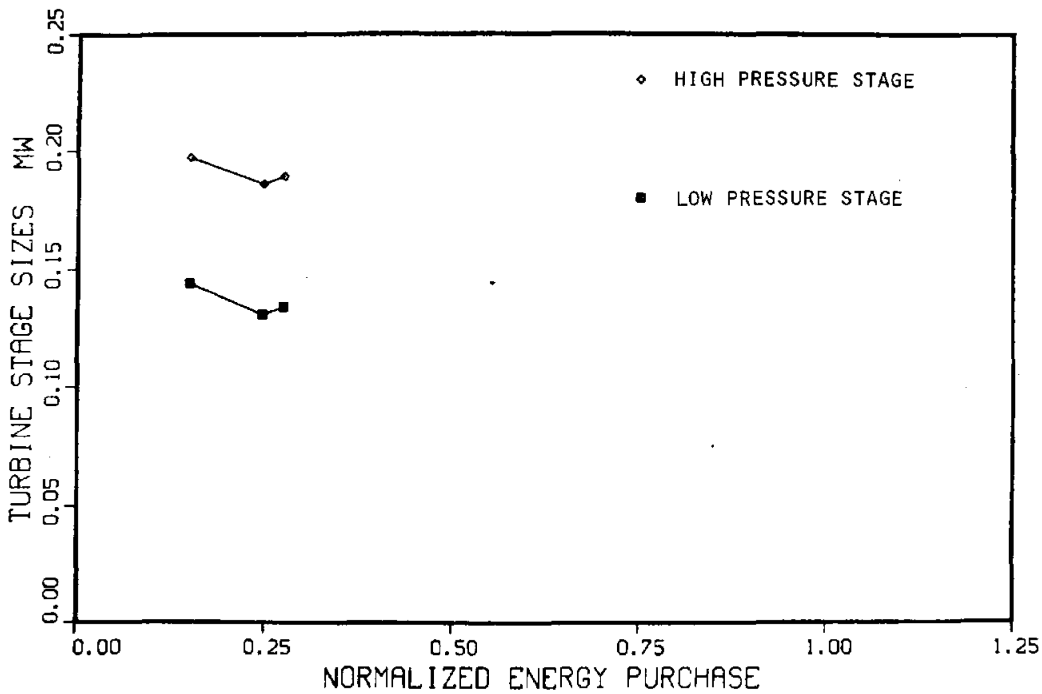

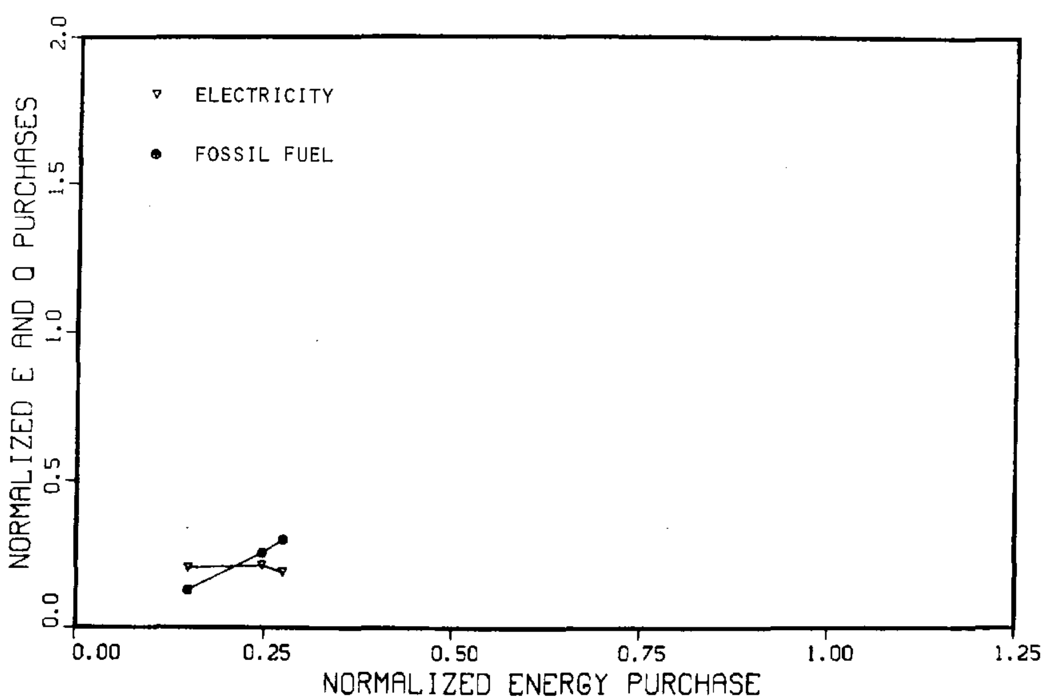

Figure 32. Results for the Albuquerque Location with the High Inflation Rate and the Time-of-Day Price Schedule for Electricity.

system is more expensive than the conventional system. This is a very important result, especially when one remembers that the results in this figure are for the standard inflation case.

The results for the high inflation, constant electricity cost case are plotted in Figures 24-26. In this case the optimum system is a STES which purchases approximately 27% as much energy as the conventional system. As expected, increasing the restriction on the amount of purchased energy increases the annualized cost; however, the increase is fairly small. The Nashville counterpart has a completely different result; here the cost increases rapidly with increasing purchased energy restrictions. This difference occurs primarily because there are more cloudy days in Nashville than in Albuquerque (see Figure 20). The effect of this difference in insolation can be seen in a comparison of Figures 12 and 25, which indicates that at Nashville increasing the restriction on purchased energy requires large increases in thermal storage size, and therefore large increases in collector field size, in order to keep the necessary amount of energy in thermal storage. In Albuquerque, the size changes are relatively small. These two units are expensive, which makes the Nashville system's annualized cost increase rapidly as the restriction on purchased energy is increased.

Figures 21-23 can be compared to Figures 27-29, and Figures 24-26 can be compared to Figures 30-32, to see the effect of time-of-day pricing. Comparison of the two standard inflation cases shows the optimum system for the time-of-day electricity pricing schedule case is a STES, while for the constant price case it is a fossil fuel total energy system. This indicates that this particular time-of-day electricity pricing schedule confers a slight advantage on STES. In all other cases the effect of the type of pricing schedule is slight.

Conclusions

The methodology described in this paper is sufficiently flexible and accurate so that it may be used to analyze many different applications. The computer code is also relatively small and fast running, and therefore, these analyses will be fairly inexpensive. Energy inflation rates and system location have a strong effect on the system design. For the case where the energy cost inflation rates are small, an STE system which begins operation in 1982 and which reduces energy consumption by 75% costs less than 1.75 times the cost of a conventional system (see Figure 8) and in some cases costs less than the conventional system (see Figure 21). This indicates STE systems could become important sources of energy for industries where the cost of energy is a small fraction of the business costs, and which wish to continue operating during energy shortages. These results are based upon high production rate costs for the major components.

REFERENCES

1. Boes, E. C., et al., "Availability of Direct, Total, and Diffuse Solar Radiation to Fixed and Tracking Collectors in the U.S.A.," SAND77-0885, Sandia Laboratories, August 1977.

2. Perino, A. M., "A Methodology for Determining the Economic Feasibility of Residential or Commercial Solar Energy Systems" SAND78-0931, Sandia Laboratories, January 1979.

3. Haskell, K. H. and Jones, R. E., "Brief Instructions for Using the Sandia Mathematical Subroutine Library," SAND77-1441, Sandia Laboratories, June 1978.

4. Iman, R. L., Helton, J. C., and Campbell, J. F., "Risk Methodology for Geologic Disposal of Radioactive Waste: Sensitivity Analysis Techniques," SAND78-0912, Sandia Laboratories, October 1978.

5. Anon., "Solar Total Energy--Large Scale Experiment #2, Phase II Conceptual Design," SD Document No. 78SDS4200, January 12, 1978.

6. Anon., "Preliminary Design of the Solar Total Energy Large Scale Experiment at Shenandoah, Georgia," Contractor Progress Report for Contract No. EG77-C-04-3985, May 1 & 2, 1978.

7. Personal Communication, J. P. Abbin, Division 2324, Sandia Laboratories, Albuquerque, NM.

8. Hall, I. J., Prairie, R. R., Anderson, H. E. and Boes, E. C., "Generation of a Typical Meteorological Year for 26 SOLMET Stations," SAND78-1601, Sandia Laboratories, August 1978.

DISTRIBUTION:

TID-4500-R66 UC-62A (288)

U.S. Department of Energy (3)
Division of Central Solar Technology
600 E Street NW
Washington, DC 20545
Attn: J. E. Rannels
G. W. Braun
M. E. Resner

U. S. Department of Energy (4)
Division of Conservation and Solar Applications
MS 2221C
Washington, DC 20545
Attn: F. Morse
J. Dollard
W. Auer
R. Bezdek

U.S. Department of Energy
San Francisco Operations Office
1333 Broadway, Wells Fargo Bldg.
Oakland, CA 94612
Attn: W. Hughey
D. Nealy

U.S. Department of Energy (3)
Albuquerque Operations Office
P. O. Box 5400
Albuquerque, NM 87185
Attn: D. K. Nowlin, Director (2)
Special Programs Div.
G. N. Pappas

Oak Ridge National Laboratory
P. O. Box Y
Oak Ridge, TN 37830
Attn: G. Lawson

Aerospace Corporation
101 Continental Blvd.
El Segundo, CA 90245
Attn: Elliott L. Katz

Jet Propulsion Laboratory
4800 Oak Grove Drive
Pasadena, CA 91103
Attn: V. C. Truscello

McDonnell Douglas Astronautics Co. - West
5301 Bolsa Avenue
Huntington Beach, CA 92647
Attn: J. Rogan, A3-374

Science Applications, Inc.
200 Lomas NW
Suite 600
Albuquerque, NM 87102
Atnn: J. M. Alcone

Solar Energy Research Institute (3)
1536 Cole Boulevard
Golden, CO 80401
Attn: K. Touryan
F. Krieth
N. Woodley

Colorado State University
Dept. of Mechanical Engineering
Fort Collins, CO 80523
Attn: P. J. Wilbur

1223 R. L. Iman
2324 J. P. Abbin
2324 R. S. Urenda
2623 E. A. Aronson
4700 J. H. Scott
4710 G. E. Brandvold
4713 B. W. Marshall
4714 R. P. Stromberg
4715 R. H. Braasch
4716 H. M. Dodd
4719 D. G. Schueler
4720 V. L. Dugan
4722 J. F. Banas
4722 R. W. Harrigan
4723 W. P. Schimmel, Jr. (5)
4723 K. D. Bergeron
4723 C. J. Chiang
4723 D. O. Lee
4723 L. L. Lukens
4723 R. R. Peters (30)
4725 J. A. Leonard
4725 R. W. Hunke
4725 J. C. Zimmerman
8326 P. J. Eicker
8266 E. A. Aas
8450 R. C. Wayne
3141 T. L. Werner (5)
3151 W. L. Garner (3)
For DOE/TIC (Unlimited Release)